

Extended Squire's transformation and its consequences for transient growth in a confined shear flow

J. John Soundar Jerome, Jean-Marc Chomaz

▶ **To cite this version:**

J. John Soundar Jerome, Jean-Marc Chomaz. Extended Squire's transformation and its consequences for transient growth in a confined shear flow. Journal of Fluid Mechanics, 2014, 744, pp.430-456. 10.1017/jfm.2014.83 . hal-00995133

HAL Id: hal-00995133

https://polytechnique.hal.science/hal-00995133

Submitted on 28 May 2014

HAL is a multi-disciplinary open access archive for the deposit and dissemination of scientific research documents, whether they are published or not. The documents may come from teaching and research institutions in France or abroad, or from public or private research centers.

L'archive ouverte pluridisciplinaire **HAL**, est destinée au dépôt et à la diffusion de documents scientifiques de niveau recherche, publiés ou non, émanant des établissements d'enseignement et de recherche français ou étrangers, des laboratoires publics ou privés.

J. Fluid Mech. (2014), *vol.* 744, *pp.* 430–456. © Cambridge University Press 2014
doi:10.1017/jfm.2014.83

Extended Squire's transformation and its consequences for transient growth in a confined shear flow

J. John Soundar Jerome† and Jean-Marc Chomaz

Laboratoire d'Hydrodynamique (LadHyX), École Polytechnique, 91128 Palaiseau, France

(Received 11 September 2013; revised 3 February 2014; accepted 5 February 2014; first published online 13 March 2014)

The classical Squire transformation is extended to the entire eigenfunction structure of both Orr–Sommerfeld and Squire modes. For arbitrary Reynolds numbers Re, this transformation allows the solution of the initial-value problem for an arbitrary three-dimensional (3D) disturbance via a two-dimensional (2D) initial-value problem at a smaller Reynolds number Re_{2D}. Its implications for the transient growth of arbitrary 3D disturbances is studied. Using the Squire transformation, the general solution of the initial-value problem is shown to predict large-Reynolds-number scaling for the optimal gain at all optimization times t with t/Re finite or large. This result is an extension of the well-known scaling laws first obtained by Gustavsson (*J. Fluid Mech.*, vol. 224, 1991, pp. 241–260) and Reddy & Henningson (*J. Fluid Mech.*, vol. 252, 1993, pp. 209–238) for arbitrary αRe, where α is the streamwise wavenumber. The Squire transformation is also extended to the adjoint problem and, hence, the adjoint Orr–Sommerfeld and Squire modes. It is, thus, demonstrated that the long-time optimal growth of 3D perturbations as given by the exponential growth (or decay) of the leading eigenmode times an extra gain representing its receptivity, may be decomposed as a product of the gains arising from purely 2D mechanisms and an analytical contribution representing 3D growth mechanisms equal to $1 + (\beta Re/Re_{2D})^2\,\mathscr{G}$, where β is the spanwise wavenumber and $\mathscr{G}$ is a known expression. For example, when the leading eigenmode is an Orr–Sommerfeld mode, it is given by the product of respective gains from the 2D Orr mechanism and an analytical expression representing the 3D lift-up mechanism. Whereas if the leading eigenmode is a Squire mode, the extra gain is shown to be solely due to the 3D lift-up mechanism. Direct numerical solutions of the optimal gain for plane Poiseuille and plane Couette flow confirm the novel predictions of the Squire transformation extended to the initial-value problem. These results are also extended to confined shear flows in the presence of a temperature gradient.

Key words: general fluid mechanics, instability, transition to turbulence

1. Introduction

For over two decades now, the linear stability analysis of shear flows has followed two lines of thought, namely, modal stability analysis and non-modal stability

† Email address for correspondence: joseph@irphe.univ-mrs.fr

analysis. The former considers solutions of the linearized Navier–Stokes equations (LNS) that grow, or decay, exponentially in time (Lin 1955; Chandrasekhar 1961; Joseph 1976; Drazin & Reid 1981), whereas the latter investigates the dynamics of disturbances over a finite-time horizon without assuming exponential time dependence (Farrell 1988; Reddy & Henningson 1993; Schmid & Henningson 2001; Schmid 2007). In the case of parallel shear flows, the celebrated Squire transformation (Squire 1933) relates any arbitrarily oriented three-dimensional (3*D*) modal solution of non-zero streamwise wavenumber at a given Reynolds number to a two-dimensional (2D) modal solution with the same total wavelength but zero spanwise wavenumber (hereafter referred to as spanwise disturbances) at a smaller Reynolds number. Since in the transformation the growth rate of 3D perturbations is smaller than that of 2D perturbations, it leads to the well-known Squire theorem which states that 2D modes are more unstable than 3D modes of the same total wavelength, implying that the modal stability analysis can be restricted to only 2D disturbances without loss of generality.

The modal stability analysis for wall-bounded parallel shear flows predicts that 2D spanwise disturbances, in the form of Tollmien–Schlichting (TS) waves, are the most unstable modes (Tollmien 1929; Schlichting 1933). Using a novel vibrating ribbon experiment, Schubauer & Skramstad (1947) measured and compared the growth rate of TS waves with the modal stability theory. Later, Klebanoff, Tidstrom & Sargent (1962) described how the onset of 2D TS instability waves can lead to 3D turbulent fluctuations. In a laminar boundary layer, they also used a vibrating ribbon to generate and follow the slow evolution of 2D TS waves in a controlled environment. As the TS wave amplitude exceeded 1 % of the free-stream velocity, they observed that the spanwise-uniform TS waves exhibit a rapid growth of spanwise variations, thereby leading to longitudinal vortices. Herbert (1988) used the Floquet theory of secondary instability to describe the evolution of such spanwise periodic disturbances from 2D TS waves. Bayly, Orszag & Herbert (1988), Kachanov (1994), Schlichting & Gersten (2000) provide a review of the resulting transition scenario and its consequences for turbulence shear flows. On the other hand, experiments in the presence of high free-stream turbulence (Morkovin 1968; Klebanoff 1971; Morkovin 1978, 1984; Kendall 1985; Matsubara & Alfredsson 2001) show that transition is usually preceded by the presence of streamwise motion in the form of streaks and not via TS waves as predicted by modal stability analysis. For example, Matsubara & Alfredsson (2001) demonstrated that a boundary layer which is subjected to free-stream turbulence levels in the range 1–6 % develops streamwise elongated regions of high and low streamwise velocity which lead to secondary instability and transition to turbulence. Such perturbation dynamics at the onset of transition have been analysed by numerous experimental and direct numerical studies confirming this so-called *bypass* transition scenario (see the review by Saric, Reed & Kerschen (2002) and references therein).

Ellingsen & Palm (1975) considered a streamwise-uniform disturbance in an inviscid shear flow to deduce that the streamwise velocity of these disturbances can grow linearly in time. They cite that it was E. Hølland who originally suggested in his lecture notes that certain 3D disturbances can grow transiently in inviscid shear flows. Landhal (1980) generalized their result to all parallel inviscid constant-density shear flows by showing that a wide range of initial infinitesimal 3D disturbances (in particular, those disturbances with a non-zero wall-normal velocity component) exhibit algebraic growth. Hultgren & Gustavsson (1981) were the first to consider such three-dimensional perturbations in the case of viscous parallel shear flows. They studied the temporal evolution of small 3D disturbances with large streamwise

wavelength (i.e. nearly streamwise-uniform) in viscous boundary layers. It was deduced that, at short time, the streamwise perturbation velocity evolves according to the inviscid initial-value problem analysed by Ellingsen & Palm (1975) and Landhal (1980). Later, viscous dissipation dominates and the disturbance eventually decays. Further studies showed that such transient growth of disturbances exists in many parallel viscous shear flows. Using a variational approach, Farrell (1988) computed the optimal 3D perturbations that give rise to the maximum possible transient growth at a given time interval. The kinetic energy of certain optimal perturbations can grow as large as $O(Re^2)$ in plane Poiseuille (Gustavsson 1991; Reddy & Henningson 1993) and plane Couette flows (Farrell & Ioannou 1993). Depending on the initial conditions and the Reynolds number, nonlinear effects may become important during the transient growth of disturbances in these flows. Waleffe (1995) proposed a self-sustaining process for turbulent shear flows consisting of finite-amplitude streamwise rolls that create nonlinear streaks via transient growth and the nonlinear streaks undergo a secondary modal instability to form wall-normal vortices that, in turn, regenerate streamwise rolls via vortex tilting. It is now widely accepted that such self-sustaining processes form the basis of the so-called bypass transition.

The process of short-time growth of disturbance kinetic energy in the absence of nonlinear effects can be associated with the non-normality of the governing linear operator (Boberg & Brosa 1988; Farrell 1988; Butler & Farrell 1992; Reddy & Henningson 1993), i.e. the non-orthogonality of the associated eigenfunctions. Even though each eigenfunction may decay at its own growth rate (related to its eigenvalue), a superposition of non-orthogonal eigenfunctions may produce large transient growth before eventually decreasing at the rate of the least stable eigenfunction. Transient growth can also occur when an eigenvalue is degenerate and the operator is non-diagonal (Gustavsson & Hultgren 1980; Shanthini 1989). For unbounded or semi-bounded shear flows, the continuous spectrum may also contribute to transient growth (Hultgren & Gustavsson 1981). But these cases are outside the scope of the present study, since we consider bounded shear flows wherein the spectrum is discrete; and we also assume the spectrum to be non-degenerate since this occurs on a set of control parameters of zero measure (Schmid & Henningson 2001).

The lift-up mechanism (Moffatt 1967; Ellingsen & Palm 1975; Landhal 1980) and the Orr mechanism (Orr 1907) are two such commonly identified disturbance growth phenomena in a shear flow. The lift-up mechanism is considered to be the dominant mechanism in many wall-bounded shear flows. According to the lift-up mechanism, an infinitesimal streamwise-uniform vortex superimposed on a parallel shear flow can lift-up low-speed fluid from the wall and push high-velocity fluid towards the wall until viscous dissipation becomes important at times of the order of the Reynolds number Re. The Orr mechanism is associated with the increase in disturbance kinetic energy due to an initial disturbance field that consists of spanwise-uniform vortices that are tilted against the direction of the base flow. Such a disturbance can grow by extracting the base-flow kinetic energy via the Reynolds stress production term. Considering plane wave solutions for arbitrary 3D perturbations, Farrell & Ioannou (1993) demonstrated that any growth in wall-normal velocity via the Orr mechanism can eventually lead to large amplification of the streamwise velocity through the lift-up mechanism. In a more recent study, Vitoshkin *et al.* (2012) explained that 3D optimal growth arises when the spanwise vorticity and the 2D spanwise divergence field are in/out phase when the mean flow shear is positive/negative.

In the case of confined viscous shear flows, disturbance growth over a finite-time horizon (or non-modal behaviour) can be computed via an eigenfunction expansion

(Schmid & Henningson 2001; Schmid 2007). In this context, the present article extends the classical Squire transformation to the wall-normal vorticity component of both the Orr–Sommerfeld and the Squire modes. The implications of this extended Squire transformation for the arbitrary initial-value problem of the LNS equation are then explored. As a result, a large-Reynolds-number transformation that relates the entire optimal gain curve of any 3D perturbation to a generic 2D problem is obtained (§ 5). The extended Squire transformation and the resulting asymptotic solution to the LNS equation at $Re \gg 1$ can be viewed as a generalization of the well-known large-Reynolds-number scaling laws first deduced by Gustavsson (1991) and Reddy & Henningson (1993) (§ 8.2).

2. Governing equations

The evolution of 3D infinitesimal disturbances in a shear flow is governed by the LNS equations with appropriate boundary conditions. For parallel shear flows that are homogeneous and infinite along streamwise (x-axis) and spanwise (z-axis) directions with base flow velocity $\boldsymbol{U} = [U_0(y), 0, 0]^{\mathrm{T}}$, the solution $\boldsymbol{q} = \left[v\,(x, y, z, t)\,,\, \eta\,(x, y, z, t)\right]^{\mathrm{T}}$ (where v and η are wall-normal velocity and vorticity perturbation components, respectively) of the LNS equations may be expanded in the so-called normal mode formulation (Lin 1955; Chandrasekhar 1961; Joseph 1976; Drazin & Reid 1981; Schmid & Henningson 2001):

$$\boldsymbol{q} = \int_0^\infty \int_0^\infty \tilde{\boldsymbol{q}}\,(y, t; \alpha, \beta)\, \mathrm{e}^{\mathrm{i}\alpha x + \mathrm{i}\beta y} \mathrm{d}\alpha\, \mathrm{d}\beta, \tag{2.1}$$

with the LNS equation for each wave vector $\boldsymbol{k} = (\alpha, \beta)^{\mathrm{T}}$ (where α and β are the streamwise and spanwise wavenumbers, respectively) given by

$$-\frac{\partial}{\partial t}\begin{bmatrix} k^2 - \mathrm{D}^2 & 0 \\ 0 & 1 \end{bmatrix} \tilde{\boldsymbol{q}} = \begin{bmatrix} L^O & 0 \\ \mathrm{i}\beta \frac{\mathrm{d}U_0}{\mathrm{d}y} & L^S \end{bmatrix} \tilde{\boldsymbol{q}}, \tag{2.2}$$

where $\mathrm{D} = \partial/\partial y$ and $k^2 = \alpha^2 + \beta^2$. The symbols L^O and L^S, respectively, denote the Orr–Sommerfeld and Squire operators (Gustavsson & Hultgren 1980; Schmid & Henningson 2001), namely,

$$L^O = \mathrm{i}\alpha U_0 \left(k^2 - \mathrm{D}^2\right) + \mathrm{i}\alpha \frac{\mathrm{d}^2 U_0}{\mathrm{d}y^2} + \frac{1}{Re}\left(k^2 - \mathrm{D}^2\right)^2, \tag{2.3}$$

$$L^S = \mathrm{i}\alpha U_0 + \frac{1}{Re}\left(k^2 - \mathrm{D}^2\right), \tag{2.4}$$

where $Re = Ul/\nu$ is the Reynolds number, with ν the kinematic viscosity, l the characteristic length scale and U the characteristic velocity scale, for the non-dimensionalization of the governing equations. For plane Poiseuille flow and plane Couette flow, l is the half-channel width $h/2$ and U is the difference in velocity between the centreline and the channel wall.

When the flow is bounded in the cross-stream direction with no-slip boundary conditions at the wall, the spectrum of (2.2) is discrete and complete (Schensted 1961; DiPrima & Habetler 1969). Considering the triangular form of the matrix

in (2.2), any solution $\tilde{\boldsymbol{q}}\,(y, t; \alpha, \beta, Re)$ at a particular wave vector of (2.2) may be expressed as

$$\tilde{\boldsymbol{q}}\,(y, t; \alpha, \beta, Re) = \sum_{j=1}^{\infty} \left(A_j^O \hat{\boldsymbol{q}}_j^O \exp(-\mathrm{i}\omega_j^O t) \right) + \sum_{j=1}^{\infty} \left(A_j^S \hat{\boldsymbol{q}}_j^S \exp(-\mathrm{i}\omega_j^S t) \right), \tag{2.5}$$

where ω_j^O and $\hat{\boldsymbol{q}}_j^O = \left[\hat{v}_j^O\,(y; \alpha, \beta, Re)\,, \hat{\eta}_j^O\,(y; \alpha, \beta, Re)\right]^{\mathrm{T}}$ are the Orr–Sommerfeld eigenvalues and eigenfunctions, respectively, with the complex frequency ω_j^O and wall-normal velocity $\hat{v}_j^O$ given by the Orr–Sommerfeld (OS) equation

$$\left(\mathrm{i}\omega_j^O (k^2 - \mathrm{D}^2) - L^O\right) \hat{v}_j^O\,(y; \alpha, \beta, Re) = 0, \tag{2.6}$$

with $\hat{v}_j^O = \mathrm{D}\hat{v}_j^O = 0$ at the wall, and the wall-normal vorticity $\hat{\eta}_j^O$ of the OS eigenfunction is given by the forced Squire (FS) equation:

$$\left(\mathrm{i}\omega_j^O - L^S\right) \hat{\eta}_j^O\,(y; \alpha, \beta, Re) = \mathrm{i}\beta \frac{\mathrm{d}U_0}{\mathrm{d}y} \hat{v}_j^O\,(y; \alpha, \beta, Re)\,, \tag{2.7}$$

with $\hat{\eta}_j^O = 0$ at the wall. The FS equation (2.7) has a solution only if ω_j^O is not in the spectrum of L^S. This condition is fulfilled except for a set of Reynolds number and wavenumber of zero measure (Schmid & Henningson 2001) and these resonant cases will not be considered here. This implies, however, that $\hat{\eta}_j^O = 0$ for 2D spanwise-uniform perturbations ($\beta = 0$). At this point, we introduce a new *auxiliary* velocity variable $\hat{\hat{\eta}}_j^O = -\mathrm{i}\hat{\eta}_j^O/\beta$ whose significance will be clear in the following sections. The corresponding forced Squire equation in terms of the OS *auxiliary velocity* is

$$\left(\mathrm{i}\omega_j^O - L^S\right) \hat{\hat{\eta}}_j^O\,(y; \alpha, \beta, Re) = \frac{\mathrm{d}U_0}{\mathrm{d}y} \hat{v}_j^O\,(y; \alpha, \beta, Re)\,, \tag{2.8}$$

with $\hat{\hat{\eta}}_j^O = 0$ at the wall. This *auxiliary velocity* $\hat{\hat{\eta}}_j^O$ has a non-zero solution when $\beta = 0$.

The Squire mode $\hat{\boldsymbol{q}}_j^S = \left[0, \hat{\eta}_j^S\,(y; \alpha, \beta, Re)\right]^{\mathrm{T}}$ does not involve wall-normal velocity. The complex frequency ω_j^S and the wall-normal vorticity $\hat{\eta}_j^S$ are solutions of the eigenvalue problem given by the Squire (SQ) equation:

$$\left(\mathrm{i}\omega_j^S - L^S\right) \hat{\eta}_j^S\,(y; \alpha, \beta, Re) = 0, \tag{2.9}$$

with $\hat{\eta}_j^S = 0$ at the wall. The coefficients $\{A_j^O\}$ and $\{A_j^S\}$ in (2.5) are determined from the initial condition.

3. The extended Squire transformation on the eigenfunctions

For the perturbations with non-zero streamwise wavenumber $\alpha \neq 0$, the OS and SQ eigenvalue problems (2.6) and (2.9) are invariant under the Squire transformation which keeps the wave-vector modulus k constant: $\alpha \to \alpha'$, $\beta \to \beta' = \sqrt{k^2 - \alpha'^2}$, $Re \to Re' = (\alpha/\alpha')\,Re$ and $\omega \to \omega' = (\alpha'/\alpha)\,\omega$. Thus, for the OS-modes, $\hat{v}_j^O \to \hat{v}_j^{O'} = \hat{v}_j^O$ and $\hat{\hat{\eta}}_j^O \to \hat{\hat{\eta}}_j^{O'} = (\alpha/\alpha')\,\hat{\hat{\eta}}_j^O$ and for the SQ-modes, $\hat{\eta}_j^S \to \hat{\eta}_j^{S'} = \hat{\eta}_j^S$. By setting $\alpha' = k$, β vanishes and any 3D eigenmode is related to a 2D spanwise eigenmode at a smaller Reynolds number $Re_{2D} = (\alpha/k)\,Re$ with a larger frequency and growth rate given by

$\omega_{2D} = (k/\alpha)\,\omega$. Implications of the classical Squire transformation are well-known for the wall-normal velocity component $\hat{v}_j^O$ of the OS-mode:

$$\hat{v}_j^O(y;\,\alpha,\,\beta,\,Re) = \hat{v}_j^{O2D}(y;\,k,\,Re_{2D}), \tag{3.1}$$

where $\hat{v}_j^{O2D}$ is the solution of the 2D Orr–Sommerfeld equation (Lin 1955; Chandrasekhar 1961; Joseph 1976; Drazin & Reid 1981; Schmid & Henningson 2001)

$$\left[\mathrm{i}\left(\omega_j^{O2D} - kU_0\right)\left(k^2 - \mathrm{D}^2\right) - \mathrm{i}k\frac{\mathrm{d}^2U_0}{\mathrm{d}y^2} - \frac{1}{Re_{2D}}\left(k^2 - D^2\right)^2\right]\hat{v}_j^{O2D}(y;\,k,\,Re_{2D}) = 0, \tag{3.2}$$

with $\hat{v}_j^{O2D} = \mathrm{D}\hat{v}_j^{O2D} = 0$ at the wall. However, to the authors' best knowledge, the transformation of the wall-normal vorticity component of the OS and SQ eigenmodes has never been considered before. Most of the results presented here are precisely due to this extension of the classical Squire transformation.

For the OS-mode the wall-normal vorticity $\hat{\eta}_j^O$ vanishes for the 2D case but the Squire transformation suggests rewriting it in terms of the *auxiliary velocity* variable as

$$\hat{\eta}_j^O(y;\,\alpha,\,\beta,\,Re) = \mathrm{i}\beta\frac{k}{\alpha}\hat{\hat{\eta}}_j^{O2D}(y;\,k,\,Re_{2D}), \tag{3.3}$$

where $\hat{\eta}_j^{O2D}$ is the solution of the 2D Squire equation forced at ω_j^{O2D}:

$$\left[\mathrm{i}\left(\omega_j^{O2D} - kU_0\right) - \frac{1}{Re_{2D}}\left(k^2 - \mathrm{D}^2\right)\right]\hat{\hat{\eta}}_j^{O2D}(y;\,k,\,Re_{2D}) = \frac{\mathrm{d}U_0}{\mathrm{d}y}\hat{v}_j^{O2D}(y;\,k,\,Re_{2D}), \tag{3.4}$$

with $\hat{\hat{\eta}}_j^{O2D} = 0$ at the wall. Applying the Squire transformation also to the wall-normal vorticity $\hat{\eta}_j^O$ is somewhat unusual, since $\hat{\eta}_j^O$ is zero in the strictly 2D case. However, the auxiliary velocity variable is non-zero when $\beta = 0$. As a result, it can be shown (see § 4) that the corresponding 2D velocity field is equivalent to a three-component 2D flow: three non-zero velocity components which are uniform in the spanwise direction. On the other hand, if 3D perturbations that are asymptotic to the longitudinal case are considered by taking $\alpha \to 0$ at constant k and Re_{2D} (i.e. assuming that the flow Reynolds number $Re = k\,Re_{2D}/\alpha$ goes to infinity), (3.3) then implies that the wall-normal vorticity $\hat{\eta}_j^O$ of the OS-mode diverges as α^{-1} while the wall-normal velocity $\hat{v}_j^O$ remains constant. This is another manifestation of the lift-up mechanism (Moffatt 1967; Ellingsen & Palm 1975; Landhal 1980; Boberg & Brosa 1988; Gustavsson 1991; Butler & Farrell 1992; Farrell & Ioannou 1993) in 3D OS-modes whereby the wall-normal vorticity $\hat{\eta}_j^O$ is a forced response due to the tilting of the base-flow shear $\mathrm{d}U_0/\mathrm{d}y$ by the wall-normal velocity $\hat{v}_j^O$ solution of the OS equation.

Similarly, for the SQ-mode the wall-normal vorticity $\hat{\eta}_j^S$ should vanish for the strictly 2D case. But if, instead, one considers the so-called three-component 2D flows wherein the spanwise velocity $\hat{w}$ is non-zero but uniform in the spanwise direction, the wall-normal vorticity is then non-zero in the 2D case and it corresponds to the variation of the spanwise velocity $\hat{w}^{S2D}$ in the streamwise direction given by

$\hat{\eta}_j^{S2D} = -\mathrm{i}k\hat{w}^{S2D}$. Then, the extended Squire transformation also applies to the Squire mode with

$$\hat{\eta}_j^{S}(y;\,\alpha,\,\beta,\,Re) = \hat{\eta}_j^{S2D}(y;\,k,\,Re_{2D}), \tag{3.5}$$

where $\hat{\eta}_j^{S2D}$ is the 2D Squire eigenfunction solution of the 2D Squire equation valid for the three-component 2D flow:

$$\left[\mathrm{i}\left(\omega_j^{S2D} - kU_0\right) - \frac{1}{Re_{2D}}\left(k^2 - \mathrm{D}^2\right)\right]\hat{\eta}_j^{S2D}(y;\,k,\,Re_{2D}) = 0, \tag{3.6}$$

with $\hat{\eta}_j^{S2D} = 0$ at the wall. Equations (3.3) and (3.5) relating $\hat{\eta}_j^{O}$ and $\hat{\eta}_j^{S}$, respectively, to the $\hat{\hat{\eta}}_j^{O2D}$ and $\hat{\eta}_j^{S2D}$ introduced here define the extended Squire transformation.

4. The extended Squire transformation in primitive variables

It is interesting to rewrite the extended Squire transformation in terms of the normal modes of the Fourier-transformed primitive variables, namely, the streamwise velocity $\hat{u}(y;\,\alpha,\,\beta,\,Re)$, the wall-normal velocity $\hat{v}(y;\,\alpha,\,\beta,\,Re)$, the spanwise velocity $\hat{w}(y;\,\alpha,\,\beta,\,Re)$ and the pressure field $\hat{p}(y;\,\alpha,\,\beta,\,Re)$. In this case, the non-dimensional governing equations of the perturbation velocity and pressure field are

$$\mathrm{i}\alpha\hat{u} + \mathrm{D}\hat{v} + \mathrm{i}\beta\hat{w} = 0, \tag{4.1}$$

$$\left[\mathrm{i}\left(\omega - \alpha U_0\right) + \frac{1}{Re}\left(\mathrm{D}^2 - k^2\right)\right]\hat{u} = \mathrm{i}\alpha\hat{p} + \hat{v}\frac{\mathrm{d}U_0}{\mathrm{d}y}, \tag{4.2}$$

$$\left[\mathrm{i}\left(\omega - \alpha U_0\right) + \frac{1}{Re}\left(\mathrm{D}^2 - k^2\right)\right]\hat{v} = \mathrm{D}\hat{p}, \tag{4.3}$$

and

$$\left[\mathrm{i}\left(\omega - \alpha U_0\right) + \frac{1}{Re}\left(\mathrm{D}^2 - k^2\right)\right]\hat{w} = \mathrm{i}\beta\hat{p}, \tag{4.4}$$

with $\hat{u} = \hat{v} = \hat{w} = \hat{p} = 0$ at the wall. The classical Squire transformation should be valid for the primitive variables as well. Thus, for each 3D normal mode ($\hat{u}$, $\hat{v}$, $\hat{w}$, $\hat{p}$), there exists a 2D spanwise-uniform normal mode at a smaller Reynolds number $Re_{2D} = (\alpha/k)\,Re$ with a larger frequency and growth rate given by $\omega_{2D} = (k/\alpha)\,\omega$. It can be verified that the following extended Squire's transformation for the primitive variables exists, for all α, β and Re:

$$\hat{u}(y;\,\alpha,\,\beta,\,Re) = \frac{k}{\alpha}\left[\hat{u}^{2D}(y;\,k,\,Re_{2D}) - \frac{\beta^2}{k^2}\hat{w}^{2D}(y;\,k,\,Re_{2D})\right], \tag{4.5}$$

$$\hat{v}(y;\,\alpha,\,\beta,\,Re) = \hat{v}^{2D}(y;\,k,\,Re_{2D}), \tag{4.6}$$

$$\hat{w}(y;\,\alpha,\,\beta,\,Re) = \frac{\beta}{k}\hat{w}^{2D}(y;\,k,\,Re_{2D}), \tag{4.7}$$

$$\hat{p}(y;\,\alpha,\,\beta,\,Re) = \frac{\alpha}{k}\hat{p}^{2D}(y;\,k,\,Re_{2D}), \tag{4.8}$$

where the governing equations corresponding to the 2D spanwise-uniform fields are

$$\mathrm{i}k\hat{u}^{2D} + \mathrm{D}\hat{v}^{2D} = 0, \tag{4.9}$$

$$\left[\mathrm{i}\left(\omega^{2D} - kU_0\right) + \frac{1}{Re_{2D}}\left(\mathrm{D}^2 - k^2\right)\right]\hat{u}^{2D} = \mathrm{i}k\hat{p}^{2D} + \hat{v}^{2D}\frac{\mathrm{d}U_0}{\mathrm{d}y}, \tag{4.10}$$

$$\left[\mathrm{i}\left(\omega^{2D} - kU_0\right) + \frac{1}{Re_{2D}}\left(\mathrm{D}^2 - k^2\right)\right]\hat{v}^{2D} = \mathrm{D}\hat{p}^{2D}, \tag{4.11}$$

and

$$\left[\mathrm{i}\left(\omega^{2D} - kU_0\right) + \frac{1}{Re_{2D}}\left(\mathrm{D}^2 - k^2\right)\right]\hat{w}^{2D} = \mathrm{i}k\hat{p}^{2D}, \tag{4.12}$$

with $\hat{u}^{2D} = \hat{v}^{2D} = \hat{w}^{2D} = \hat{p}^{2D} = 0$ at the wall. Equations (4.9)–(4.11) are the commonly known Squire-transformed 2D-equivalent of (4.1)–(4.3) for the streamwise and wall-normal velocity components. The Squire transformation for the $\hat{u}$-component (4.5) shows a complex behaviour related to the contributions from the 2D streamwise and spanwise velocity components with different scalings. Together with the transformation for $\hat{w}$ (4.7) and the evolution equation of $\hat{w}^{2D}$, they can be considered as an extension to the classical Squire transformation. In this way, every 3D perturbation field can be related to a three-component 2D perturbation field.

The 2D spanwise velocity $\hat{w}^{2D}$ is, by definition, independent of β. As $\beta \to 0$ ($\alpha \to k$), from (4.5) we obtain that $\hat{u} \to \hat{u}^{2D}$ and from (4.7), we get

$$\lim_{\beta \to 0} \frac{\hat{w}}{\beta} = \frac{\hat{w}^{2D}}{k}. \tag{4.13}$$

If $[\hat{u}_j^{S2D},\ \hat{v}_j^{S2D},\ \hat{w}_j^{S2D},\ \hat{p}_j^{S2D}]^{\mathrm{T}}$ denotes the 2D SQ-mode in primitive variables, the wall-normal velocity $\hat{v}_j^{S2D}$ is zero for the 2D SQ-mode; its streamwise velocity $\hat{u}_j^{S2D}$ and pressure field $\hat{p}_j^{S2D}$ should also be zero, according to (4.9)–(4.11). Therefore, the 2D SQ-mode in terms of the primitive variables is $[0, 0, \hat{w}_j^{S2D}, 0]^{\mathrm{T}}$ which corresponds simply to a pressure-less 2D perturbation field with only a spanwise velocity. This non-zero spanwise velocity component is uniform in the spanwise direction but varies along the streamwise and wall-normal directions.

If $[\hat{u}_j^{O2D}, \hat{v}_j^{O2D}, \hat{w}_j^{O2D}, \hat{p}_j^{O2D}]^{\mathrm{T}}$ denotes the 2D OS-mode in primitive variables, the wall-normal vorticity of any OS-mode is then

$$\hat{\eta}_j^O = \mathrm{i}\beta\frac{k}{\alpha}\left(\hat{u}_j^{O2D} - \hat{w}_j^{O2D}\right) = \mathrm{i}\beta\frac{k}{\alpha}\hat{\hat{\eta}}_j^{O2D} \tag{4.14}$$

in accordance with (3.3).

Indeed, by definition, the OS wall-normal vorticity $\hat{\eta}_j^O$ is given by $\hat{\eta}_j^O = \mathrm{i}\beta\hat{u}_j^O - \mathrm{i}\alpha\hat{w}_j^O$. The auxiliary velocity variable $\hat{\hat{\eta}}_j^O$ introduced in the previous section is then

$$\hat{\hat{\eta}}_j^O(y;\alpha,\beta,Re) = \hat{u}_j^O(y;\alpha,\beta,Re) - \frac{\alpha}{\beta}\hat{w}_j^O(y;\alpha,\beta,Re), \tag{4.15}$$

which can be rewritten using the extended Squire transformation (4.5) and (4.7) as

$$\hat{\hat{\eta}}_j^O(y;\alpha,\beta,Re) = \frac{k}{\alpha}\left[\hat{u}_j^{O2D}(y;k,Re_{2D}) - \hat{w}_j^{O2D}(y;k,Re_{2D})\right], \tag{4.16}$$

showing that

$$\hat{\hat{\eta}}_j^{O2D}(y;\alpha,\beta,Re) = \hat{u}_j^{O2D}(y;k,Re_{2D}) - \hat{w}_j^{O2D}(y;k,Re_{2D}). \tag{4.17}$$

This implies that the 2D auxiliary velocity variable represents the difference between the 2D streamwise and spanwise velocity components.

5. The extended Squire transformation on the initial-value problem

The difference in the scaling of $\hat{v}_j^O$, $\hat{\eta}_j^O$ and $\hat{\eta}_j^S$ when applying the extended Squire transformation implies that the general solution (2.5) to the initial-value problem (2.2) with the same initial condition $\tilde{\boldsymbol{q}}_0$ for various α, β and Re corresponding to the same Re_{2D} and k, can be rewritten as

$$\begin{aligned}\tilde{\boldsymbol{q}}\,(y,t;\alpha,\beta,Re) \;=\; & \sum_{j=1}^{\infty} A_j^O \begin{bmatrix} \hat{v}_j^{O2D}\,(y;k,Re_{2D}) \\ \left(\frac{\mathrm{i}\beta Re}{Re_{2D}}\right)\hat{\eta}_j^{O2D}\,(y;k,Re_{2D}) \end{bmatrix} \exp\!\left(-\mathrm{i}Re_{2D}\omega_j^{O2D}\frac{t}{Re}\right) \\ & + \sum_{j=1}^{\infty}\left(\frac{Re}{Re_{2D}}B_j^O + B_j^S\right)\begin{bmatrix} 0 \\ \hat{\eta}_j^{S2D}\,(y;k,Re_{2D}) \end{bmatrix} \\ & \times \exp\!\left(-\mathrm{i}Re_{2D}\omega_j^{S2D}\frac{t}{Re}\right). \end{aligned} \tag{5.1}$$

Here, A_j^O, B_j^O and B_j^S are constants and depend only on the initial condition $\tilde{\boldsymbol{q}}_0$ for a given k and Re_{2D}. Since the Squire modes do not contribute to the disturbance wall-normal velocity, the v-component of the initial-value $\tilde{\boldsymbol{q}}_0$, namely $\tilde{v}_0$, determines the coefficients A_j^O of the OS-modes:

$$\sum_{j=1}^{\infty} A_j^O \hat{v}_j^{O2D} = \tilde{v}_0. \tag{5.2}$$

Consequently, the coefficients A_j^S of the Squire modes play a two-fold role:

(a) One part of A_j^S should cancel the wall-normal vorticity contribution from the OS-mode and scale as Re/Re_{2D}, i.e.

$$\sum_{j=1}^{\infty} B_j^O \hat{\eta}_j^{S2D} = -\mathrm{i}\beta \sum_{j=1}^{\infty} A_j^O \hat{\eta}_j^{O2D}, \tag{5.3}$$

which is non-zero as long as $\beta \neq 0$.

(b) The other part of A_j^S should contribute to the initial wall-normal vorticity field $\tilde{\eta}_0$ of $\tilde{\boldsymbol{q}}_0$

$$\sum_{j=1}^{\infty} B_j^S \hat{\eta}_j^{S2D} = \tilde{\eta}_0. \tag{5.4}$$

This may be proved by considering a given Re_{2D} and k, as Re changes. For $t \ll Re/Re_{2D}$, the short-time expansion of wall-normal vorticity in the solution (5.1) gives

$$\tilde{\eta}\,(y,t;k,Re_{2D}) = \Pi_0 + k\Pi_1 t - \mathrm{i}Re_{2D}\Pi_2\frac{t}{Re} + O\left(t^2\right), \tag{5.5}$$

where

$$\Pi_0 \;=\; \frac{Re}{Re_{2D}}\sum_{j=1}^{\infty}\left(\mathrm{i}\beta A_j^O\hat{\eta}_j^{O2D} + B_j^O\hat{\eta}_j^{S2D}\right) + \sum_{j=1}^{\infty} B_j^S\hat{\eta}_j^{S2D}, \tag{5.6}$$

$$\Pi_1 = \sum_{j=1}^{\infty} \left(\frac{\beta}{k} A_j^O \hat{\tilde{\eta}}_j^{O2D} \omega_j^{O2D} - \frac{\mathrm{i}}{k} B_j^O \hat{\eta}_j^{S2D} \omega_j^{S2D} \right), \tag{5.7}$$

and

$$\Pi_2 = \sum_{j=1}^{\infty} B_j^S \hat{\eta}_j^{S2D} \omega_j^{S2D}. \tag{5.8}$$

Since $\tilde{\eta}_0(y)$ is assumed to be the same for all Re,

$$\sum_{j=1}^{\infty} \left(\mathrm{i}\beta A_j^O \hat{\tilde{\eta}}_j^{O2D} + B_j^O \hat{\eta}_j^{S2D} \right) = 0, \tag{5.9}$$

and hence,

$$\sum_{j=1}^{\infty} B_j^S \hat{\eta}_j^{S2D} = \tilde{\eta}_0, \tag{5.10}$$

showing that the initial vorticity $\tilde{\eta}_0$ is only spanned by the Squire modes $\hat{\eta}_j^{S2D}$.

As Re becomes very large, the leading term for $1 \ll t \ll Re/Re_{2D}$ is

$$\tilde{\eta}(y, t; k, Re_{2D}) \sim k\Pi_1 t, \tag{5.11}$$

which offers the possibility for short-time growth even if ω_j^O and ω_j^S are all stable with negative imaginary parts. Since the kinetic energy of the disturbance E_k, in terms of wall-normal velocity and vorticity, reads

$$E_k(t) = \frac{1}{2} \int_{-1}^{1} \left[|\tilde{v}|^2 + k^{-2} \left(|\mathrm{D}\tilde{v}|^2 + |\tilde{\eta}|^2 \right) \right] \mathrm{d}y, \tag{5.12}$$

where, with no loss of generality, the y-domain is assumed to be bounded by $y = \pm 1$ for convenience. For $1 \ll t \ll Re/Re_{2D}$, the energy is led by the η-term in (5.12), giving

$$E_k(t) \sim \frac{t^2}{2} \int_{-1}^{1} |\Pi_1|^2 \, \mathrm{d}y. \tag{5.13}$$

The optimal growth is obtained by solving for an initial disturbance that would give rise to the maximum possible growth at a particular time horizon t and it is defined by the gain function

$$G(t; \alpha, \beta, Re) = \sup_{\forall E_k(0) \neq 0} \frac{E_k(t)}{E_k(0)}, \tag{5.14}$$

where $E_k(0)$ is the initial perturbation kinetic energy. For fixed Re_{2D} and k, the intermediate-time asymptotics at $1 \ll t \ll Re/Re_{2D}$, for Re going to infinity gives

$$G(t; \alpha, \beta, Re) \sim \left(\frac{Re}{Re_{2D}} \right)^2 t_{2D}^2 \mathscr{G}_{2D}(k, Re_{2D}), \tag{5.15}$$

with $t_{2D} = tRe_{2D}/Re$ and

$$\mathscr{G}_{2D}\,(k, Re_{2D}) = \sup_{\forall E_k(0)\neq 0} \left[\frac{\frac{1}{2}\int_{-1}^{1} |\Pi_1|^2 \,\mathrm{d}y}{E_k(0)} \right], \tag{5.16}$$

which is a function of k and Re_{2D}, independent of time and Reynolds number Re, since Π_1 depends only on A_j^O, $\hat{\hat{\eta}}_j^{O2D}$, ω_j^{O2D}, B_j^O, $\hat{\eta}_j^{S2D}$ and ω_j^{S2D}. Furthermore, Π_1 is independent of B_j^S and maximizing $\mathscr{G}_{2D}$ then imposes $B_j^S = 0$ which gives $\tilde{\eta}_0(y) = 0$. Thus, the optimal in (5.16) should be looked for within initial conditions on $\tilde{v}_0(y)$ only.

For time $t \gtrsim Re/Re_{2D}$, the large-Reynolds-number Re asymptotics for the energy is given by

$$E_k(t) \sim \left(\frac{Re}{Re_{2D}}\right)^2 \mathscr{I}_{2D}\,(t_{2D}; k, Re_{2D})\,, \tag{5.17}$$

where

$$\begin{aligned}\mathscr{I}_{2D}(t_{2D}; kRe_{2D}) \;=\; & \frac{1}{2}\int_{-1}^{1} \left| \sum_{j=1}^{\infty} \left(A_j^O \hat{\hat{\eta}}_j^{O2D} \exp[-\mathrm{i}\omega_j^{O2D} t_{2D}] \right.\right. \\ & \left.\left. -\; \frac{\mathrm{i}}{k} B_j^O \hat{\eta}_j^{S2D} \exp[-\mathrm{i}\omega_j^{S2D} t_{2D}] \right) \right|^2 \mathrm{d}y. \end{aligned} \tag{5.18}$$

The integral $\mathscr{I}_{2D}\,(t_{2D}; k, Re_{2D})$ vanishes only at $t_{2D} = 0$ and is $O\left(|\exp\left(-2\mathrm{i}\omega_{\max}^{2D} t_{2D}\right)|\right)$, where $\omega_{\max}^{2D}$ is the leading eigenvalue among ω_j^{O2D} and ω_j^{S2D} when t_{2D} is large. Thus, the large-time asymptotics using the extended Squire transformation imposes that

$$G\,(t; \alpha, \beta, Re) \sim \left(\frac{Re}{Re_{2D}}\right)^2 G_{2D}\,(t_{2D}; k, Re_{2D})\,, \tag{5.19}$$

with

$$G_{2D}\,(t_{2D}; k, Re_{2D}) = \sup_{\forall \tilde{E_k}(0)\neq 0} \left[\frac{\mathscr{I}_{2D}\,(t_{2D}; k, Re_{2D})}{E_k(0)} \right]. \tag{5.20}$$

Since $\mathscr{I}_{2D}\,(t_{2D}; k, Re_{2D})$ is the function (5.18) independent of the coefficients B_j^S, it depends only on the initial wall-normal velocity and since, maximizing the gain imposes the minimizing of $E_k(0)$ at constant $\mathscr{I}_{2D}\,(t_{2D}; k, Re_{2D})$, the initial wall-normal vorticity $\tilde{\eta}_0$ should be set to zero. The optimal for G_{2D} should be sought only in the initial perturbations field $\tilde{v}_0(y)$ as in the previous case when $1 \ll t \ll Re/Re_{2D}$.

The extended Squire transformation, therefore, predicts according to (5.15) and (5.19) that, as soon as $t \gg 1$ (even if $t/Re \ll 1$), the entire optimal gain curve at large Re ($\alpha \to 0$) is a unique curve dependent only on Re_{2D} and k given by $t_{2D}^2 \mathscr{G}_{2D}$ at small t_{2D} and $G_{2D}\,(t_{2D}; k, Re_{2D})$ at t_{2D} of order unity or large, once the gain is rescaled by $(Re_{2D}/Re)^2$ and the time by (Re_{2D}/Re). It also implies that the optimal initial perturbations for optimization time t large or t_{2D} arbitrary (small or large) involve only the $\tilde{v}_0(y)$ component, i.e. $\tilde{\eta}_0(y) = 0$. As we will see in § 8, this result may be seen as an extension and an alternative formal proof of the classical scaling argument put forward by Gustavsson (1991), Reddy & Henningson (1993).

6. The Squire transformation extended to the adjoint problem

The optimal gain can be analysed in a different limit, i.e. for finite Re but as time t goes to infinity, by introducing the adjoint equations with respect to the scalar product associated with the energy norm $\langle \hat{\boldsymbol{q}}_1,\ \hat{\boldsymbol{q}}_2 \rangle = \int_{-1}^{1} \hat{\boldsymbol{q}}_2^H \boldsymbol{M} \hat{\boldsymbol{q}}_1 \mathrm{d}y$, where superscript H represents the conjugate-transpose of a matrix and $\boldsymbol{M} = k^{-2} \begin{bmatrix} (k^2 - \mathrm{D}^2) & 0 \\ 0 & 1 \end{bmatrix}$. The norm with respect to this scalar product is related to the kinetic energy defined in (5.12) as $E_k(t) = \frac{1}{2} \|\tilde{\boldsymbol{q}}\|^2$. Thus, the adjoint equations are

$$-\frac{\partial}{\partial t} \begin{bmatrix} k^2 - \mathrm{D}^2 & 0 \\ 0 & 1 \end{bmatrix} \tilde{\boldsymbol{q}}^\dagger = \begin{bmatrix} L^{O\dagger} & -\mathrm{i}\beta \frac{\mathrm{d}U_0}{\mathrm{d}y} \\ 0 & L^{S\dagger} \end{bmatrix} \tilde{\boldsymbol{q}}^\dagger, \tag{6.1}$$

where $L^{O\dagger}$ and $L^{S\dagger}$ represent the adjoint Orr–Sommerfeld and Squire operators, respectively,

$$L^{O\dagger} = -\mathrm{i}\alpha U_0 \left(k^2 - \mathrm{D}^2\right) + 2\mathrm{i}\alpha \frac{\mathrm{d}U_0}{\mathrm{d}y} \mathrm{D} + \frac{1}{Re} \left(k^2 - D^2\right)^2, \tag{6.2}$$

$$L^{S\dagger} = -\mathrm{i}\alpha U_0 + \frac{1}{Re} \left(k^2 - \mathrm{D}^2\right), \tag{6.3}$$

and the adjoint state vector is $\tilde{\boldsymbol{q}}^\dagger = [\tilde{v}^\dagger\ (y, t; \alpha, \beta, Re)\ ,\ \tilde{\eta}^\dagger\ (y, t; \alpha, \beta, Re)]^{\mathrm{T}}$. Here, $\tilde{v}^\dagger(y, t;\ \alpha, \beta, Re)$ and $\tilde{\eta}^\dagger\ (y, t; \alpha, \beta, Re)$ denote the adjoint wall-normal velocity and vorticity components, respectively. The spectrum of the adjoint OS-operator $L^{O\dagger}$ is the complex conjugate of the spectrum of the direct OS-operator L^O and similarly for the adjoint SQ-operator $L^{S\dagger}$. But in the adjoint linear operator (6.1), it is the wall-normal vorticity $\tilde{\eta}^\dagger$ that forces the adjoint wall-normal velocity equation whereas the adjoint Squire equation is independent of the adjoint wall-normal velocity $\tilde{v}_j^\dagger$. The adjoint OS-modes $\hat{\boldsymbol{q}}_j^{O\dagger} = \left[\hat{v}_j^{O\dagger}, 0\right]^{\mathrm{T}}$ correspond then to zero wall-normal vorticity and the adjoint SQ-modes $\hat{\boldsymbol{q}}_j^{S\dagger} = \left[\hat{v}_j^{S\dagger}, \hat{\eta}_j^{S\dagger}\right]^{\mathrm{T}}$ have a non-zero wall-normal velocity corresponding to the forcing of the adjoint OS-operator by the off-diagonal term $-\mathrm{i}\beta(\mathrm{d}U_0/\mathrm{d}y)\hat{\eta}_j^{S\dagger}$ in the adjoint equation (6.1).

The Squire transformation also applies to the homogeneous part of the adjoint Orr–Sommerfeld equation and to the adjoint Squire equation. Thus, a 3D adjoint OS-mode at any α, β and Re, is related to a 2D adjoint OS-mode at $\alpha_{2D} = k$, $\beta_{2D} = 0$ and Re_{2D} via the transformation

$$\omega_j^{O*}(\alpha, \beta, Re) = \frac{\alpha}{k} \omega_j^{O2D*}\ (k, Re_{2D})\ , \tag{6.4}$$

$$\hat{v}_j^\dagger(y; \alpha, \beta, Re) = \hat{v}_j^{O2D\dagger}(y; k, Re_{2D}). \tag{6.5}$$

Similarly, the adjoint SQ-mode at any α, β and Re reads

$$\omega_j^{S*}(\alpha, \beta, Re) = \frac{\alpha}{k} \omega_j^{S2D*}\ (k, Re_{2D})\ , \tag{6.6}$$

$$\hat{\eta}_j^{S^\dagger}(y; \alpha, \beta, Re) = \hat{\eta}_j^{S2D\dagger}(y; k, Re_{2D}), \tag{6.7}$$

$$\hat{v}_j^{S\dagger}(y; \alpha, \beta, Re) = \beta \frac{k}{\alpha} \hat{v}_j^{S2D\dagger}(y; k, Re_{2D}), \tag{6.8}$$

where $\hat{v}_j^{S2D\dagger}$ is the rescaled wall-normal velocity that satisfies the 2D adjoint Orr–Sommerfeld equation forced at the complex frequency ω_j^{S2D*} by the adjoint SQ-modes such that

$$\left[\mathrm{i}(\omega_j^{S2D*} + kU_0)(k^2 - \mathrm{D}^2) - 2\mathrm{i}k\frac{\mathrm{d}U_0}{\mathrm{d}y}\mathrm{D} - \frac{1}{Re_{2D}}(k^2 - \mathrm{D}^2)^2\right]\hat{v}_j^{S2D\dagger}(y; k, Re_{2D}) = -\mathrm{i}\frac{\mathrm{d}U_0}{\mathrm{d}y}\hat{\eta}_j^{S2D\dagger}(y; k, Re_{2D})\,. \tag{6.9}$$

Thus, the Squire transformation extended to the adjoint modes predicts that the adjoint Squire mode should have a $\hat{v}^\dagger$-component scaling like Re/Re_{2D}.

7. Consequences for long-time optimal gains

Since the basis of direct modes is biorthogonal to the basis of adjoint modes (Schmid & Henningson 2001), the coefficients in the eigenfunction expansion (2.5) of the initial-value problem (2.2) for the wave vector $\boldsymbol{k} = (\alpha, \beta)$ at Re are given by:

$$A_j^O = \frac{\langle\tilde{\boldsymbol{q}}_0, \hat{\boldsymbol{q}}_j^{O\dagger}\rangle}{\langle\hat{\boldsymbol{q}}_j^O, \hat{\boldsymbol{q}}_j^{O\dagger}\rangle} \quad \text{and} \quad A_j^S = \frac{\langle\tilde{\boldsymbol{q}}_0, \hat{\boldsymbol{q}}_j^{S\dagger}\rangle}{\langle\hat{\boldsymbol{q}}_j^S, \hat{\boldsymbol{q}}_j^{S\dagger}\rangle}, \tag{7.1}$$

where $A_j^S = \left((\beta Re/Re_{2D})B_j^O + B_j^S\right)$. For $t \gg (\Delta\omega_{max})^{-1}$, where $\Delta\omega_{max}$ is the difference in the growth rate of the first and the second leading eigenmode, the long-time response is dominated by the leading eigenmode with a non-zero co-efficient in the solution (2.5).

Consider the case where the leading mode is the OS-mode $\hat{\boldsymbol{q}}_1^O = [\hat{v}_1^O, \hat{\eta}_1^O]^{\mathrm{T}}$, then at $t \gg (\Delta\omega_{max})^{-1}$, $\tilde{\boldsymbol{q}}(t) \sim A_1^O\hat{\boldsymbol{q}}_1^O\exp\left(-\mathrm{i}\omega_1^O t\right)$ and the optimization problem for long-time gain reduces to maximizing the coefficient A_1^O. Expression (7.1) shows classically that the large-time gain is achieved by taking the leading adjoint OS-mode $\hat{\boldsymbol{q}}_1^{O\dagger} = [\hat{v}_1^{O\dagger}(y), 0]^{\mathrm{T}}$ as the initial condition. Hence, the gain reads

$$G(\alpha, \beta, t; Re) \sim G_\infty^O\left|\exp^{(-2\mathrm{i}\omega_1^O t)}\right| \quad \text{with } G_\infty^O = \frac{\left\|\hat{\boldsymbol{q}}_1^O\right\|^2\left\|\hat{\boldsymbol{q}}_1^{O\dagger}\right\|^2}{\left|\langle\hat{\boldsymbol{q}}_1^O, \hat{\boldsymbol{q}}_1^{O\dagger}\rangle\right|^2}, \tag{7.2}$$

where $G_\infty^O(\alpha, \beta, t; Re)$ is the extra gain compared to the exponential variation. Similarly, if the leading eigenmode is the SQ-mode $\hat{\boldsymbol{q}}_1^S = [0, \hat{\eta}_1(y)]^{\mathrm{T}}$, $G_\infty^S = \left\|\hat{\boldsymbol{q}}_1^S\right\|^2\left\|\hat{\boldsymbol{q}}_1^{S\dagger}\right\|^2/|\langle\hat{\boldsymbol{q}}_1^S, \hat{\boldsymbol{q}}_1^{S\dagger}\rangle|^2$ denotes the extra gain compared to the exponential growth, or decay $|\exp(-2\mathrm{i}\omega_1^S t)|$.

When $\alpha \neq 0$, the extended Squire transformation states, as demonstrated in §§ 3 and 6, that, for fixed $k = \sqrt{\alpha^2 + \beta^2}$ and Re_{2D}, the direct and the adjoint OS-modes transform as

$$\hat{\boldsymbol{q}}_j^O = \begin{bmatrix}\hat{v}_j^{O2D} \\ (\mathrm{i}\beta Re/Re_{2D})\,\hat{\hat{\eta}}_j^{O2D}\end{bmatrix} \quad \text{and} \quad \hat{\boldsymbol{q}}_j^{O\dagger} = \begin{bmatrix}\hat{v}_j^{O2D\dagger} \\ 0\end{bmatrix}, \tag{7.3}$$

with $\beta = k\sqrt{1 - Re_{2D}^2/Re^2}$. Therefore, according to the extended Squire transformation, the long-time extra gain $G_\infty^O(\alpha, \beta, Re)$ may be rewritten as a product of 2D and 3D

long-time extra gains:

$$G_\infty^{O}(\alpha,\beta,Re) = G_\infty^{O2D}(k,Re_{2D})\left(1+\frac{\beta^2Re^2}{Re_{2D}^2}G_\infty^{O3D}(k,Re_{2D})\right), \tag{7.4}$$

with $G_\infty^{O2D}(k,Re_{2D}) = \left\|\hat{\boldsymbol{q}}_1^{O2D}\right\|^2\left\|\hat{\boldsymbol{q}}_1^{O2D\dagger}\right\|^2/|\langle\hat{\boldsymbol{q}}_1^{O2D},\ \hat{\boldsymbol{q}}_1^{O2D\dagger}\rangle|^2$ given by

$$G_\infty^{O2D}(k,Re_{2D}) = \frac{\displaystyle\int_{-1}^{1}\left(\left|\hat{v}_1^{O2D}\right|^2+k^{-2}\left|\mathrm{D}\hat{v}_1^{O2D}\right|^2\right)\mathrm{d}y\int_{-1}^{1}\left(\left|\hat{v}_1^{O2D\dagger}\right|^2+k^{-2}\left|\mathrm{D}\hat{v}_1^{O2D\dagger}\right|^2\right)\mathrm{d}y}{\left|\displaystyle\int_{-1}^{1}\left(\hat{v}_1^{O2D\dagger *}\hat{v}_1^{O2D}+k^{-2}\mathrm{D}\hat{v}_1^{O2D\dagger *}\mathrm{D}\hat{v}_1^{O2D}\right)\mathrm{d}y\right|^2} \tag{7.5}$$

and

$$G_\infty^{O3D}(k,Re_{2D}) = \frac{k^{-2}\displaystyle\int_{-1}^{1}\left|\hat{\hat{\eta}}_1^{O2D}\right|^2\mathrm{d}y}{\displaystyle\int_{-1}^{1}\left(\left|\hat{v}_1^{O2D}\right|^2+k^{-2}\left|\mathrm{D}\hat{v}_1^{O2D}\right|^2\right)\mathrm{d}y}, \tag{7.6}$$

where all fields are evaluated for k and Re_{2D} and here (and also hereafter) they were written without the explicit dependence for the sake of brevity. The $G_\infty^{O2D}(k,Re_{2D})$ is the extra gain that would be obtained in the 2D case and it is known to result from the classical Orr mechanism. The term $\left(\beta^2Re^2/Re_{2D}^2\right)G_\infty^{O3D}(k,Re_{2D})$ is the extra gain from the 3D-effect, the contribution to the optimal transient growth arising from the lift-up mechanism due to the forcing of the wall-normal vorticity by the wall-normal velocity. Furthermore, the extended Squire transformation explains the form of the 3D contribution $\left(1+(\beta^2Re^2/Re_{2D}^2)G_\infty^{O3D}(k,Re_{2D})\right)$ with $G_\infty^{O3D}(k,Re_{2D})$ that depends only on 2D eigenfunctions $\hat{v}_1^{O2D}$ and $\hat{\hat{\eta}}_1^{O2D}$ introduced in § 3. Contrary to the previous section where equations (5.15) and (5.19) were the large-Reynolds-number asymptotic for the gain curve valid for all times via the extended Squire transform, the present prediction (7.4) is valid for arbitrary Reynolds number but only for large time $tRe_{2D}/Re \gg 1$.

Similarly, for the direct and adjoint Squire modes the extended Squire transformation, as already demonstrated, gives

$$\hat{\boldsymbol{q}}_j^{S} = \begin{bmatrix}0\\ \hat{\eta}_j^{S2D}\end{bmatrix} \quad\text{and}\quad \hat{\boldsymbol{q}}_j^{S\dagger} = \begin{bmatrix}\beta Re/Re_{2D}\hat{v}_j^{S2D\dagger}\\ \hat{\eta}_j^{S2D\dagger}\end{bmatrix}. \tag{7.7}$$

Using this, the long-time extra gain can be rewritten as

$$G_\infty^{S}(\alpha,\beta,Re) = G_\infty^{S2D}(k,Re_{2D})\left(1+\left(\frac{\beta Re}{Re_{2D}}\right)^2G_\infty^{S3D}(k,Re_{2D})\right), \tag{7.8}$$

where

$$G_\infty^{S2D}(k,Re_{2D}) = \frac{\displaystyle\int_{-1}^{1}\left|\hat{\eta}_1^{S2D}\right|^2\mathrm{d}y\int_{-1}^{1}\left|\hat{\eta}_1^{S2D\dagger}\right|^2\mathrm{d}y}{\left|\displaystyle\int_{-1}^{1}\hat{\eta}_1^{S2D\dagger *}\hat{\eta}_1^{S2D}\mathrm{d}y\right|^2} \tag{7.9}$$

is the 2D extra gain for the 2D Squire mode which will be found numerically (see the results discussed in the next section) to be close to unity for all k and Re_{2D}. The rescaled contribution G_∞^{S3D} corresponds to the lift-up phenomenon when seen as an initial value given by the adjoint SQ-mode which has a $\beta Re/Re_{2D}$ larger $\hat{v}$-component than the $\hat{\eta}$-component:

$$G_\infty^{S3D}(k, Re_{2D}) = \frac{\displaystyle\int_{-1}^{1} \left(\left|\hat{v}_1^{S2D\dagger}\right|^2 + k^{-2} \left|\mathrm{D}\hat{v}_1^{S2D\dagger}\right|^2 \right) \mathrm{d}y}{\displaystyle k^{-2} \int_{-1}^{1} \left|\hat{\eta}_1^{S2D\dagger}\right|^2 \mathrm{d}y}. \tag{7.10}$$

Thus, the extra gain for both OS and SQ modes exhibits a lift-up contribution scaling like $\beta^2 Re^2/Re_{2D}^2$ when $Re \gg 1$ (note that $\beta = k\sqrt{1-(Re_{2D}/Re)^2}$ and $\alpha = kRe_{2D}/Re$ in the Squire transformation). No matter whether the OS-mode or SQ-mode is the least stable eigenmode, only the OS-mode exhibits a 2D extra gain due to the Orr mechanism that, as we shall see, explains why this mode determines the maximum transient growth.

8. Discussion

8.1. *Direct computations of optimal growth in plane Poiseuille and Couette flows*

Figure 1 displays optimal growth curves $G(t)$ (solid lines) directly computed using singular value decomposition (SVD) as in Jerome, Chomaz & Huerre (2012), for various Reynolds numbers Re and wavenumbers (α, β) corresponding to the same $Re_{2D} = 1000$ and $k = 1$. The analytical predictions of the optimal long-time gains $G_\infty^O|\exp(-2\mathrm{i}\omega_1^O t)|$, $G_\infty^S|\exp(-2\mathrm{i}\omega_1^S t)|$ of the leading OS- and SQ-modes computed using (7.4) and (7.8) (dashed and dashed-dotted lines, respectively) at $Re = 10^6$ corresponding to $\alpha = 10^{-3}$ are also presented in the figure. The optimal growth at any time t/Re increases with decreasing streamwise wavenumber α and after $t/Re \sim 0.03$, all optimal growth curves show two consecutive exponential decays (straight lines). In figure 1, this two-step long-time dynamics can be identified with exponential decay of the leading OS-mode and SQ-mode. Their corresponding long-time optimal gains increase as Re increases and α decreases as predicted by the scaling laws obtained using the extended-Squire transformation in §§ 5 and 7. The two-step long-time behaviour occurs because G_∞^O is larger than G_∞^S, a property retrieved for all the cases studied. When the leading eigenmode is an OS-mode, it dominates the optimal dynamics for all times large than $0.03Re$ and the piecewise exponential decay is not observed. Whereas, when the leading eigenmode is a SQ-mode, the OS-mode dominates after $t = 0.03Re$ but, since it decays faster than the SQ-mode, it is superseded after some time $\left(\log G_\infty^O - \log G_\infty^S\right)/\Delta\omega_{max}$ leading to the two-step optimal gain curve displayed in figure 1. On figure 1, it is also plotted as a dotted line, the optimal gain for the longitudinal mode $\alpha = 0$ which is to be compared with the curve for $\alpha = 10^{-3}$ at the same $Re = 10^6$. The short-time behaviour is identical but after $t = 0.02Re$, the two curves split apart as the gain for the strictly longitudinal mode keeps increasing for a much longer time, thereby depicting the singularity of the longitudinal modes. It is also observed that G_∞^O, given by the product of long-time optimal gain corresponding to the 2D Orr mechanism G_∞^{O2D} and 3D optimal gain from the lift-up mechanism $\left(Re_{2D}^2/\beta^2 Re^2\right) G_\infty^{O3D}$, is approximately the maximum optimal growth for all Reynolds numbers and wavenumbers shown here.

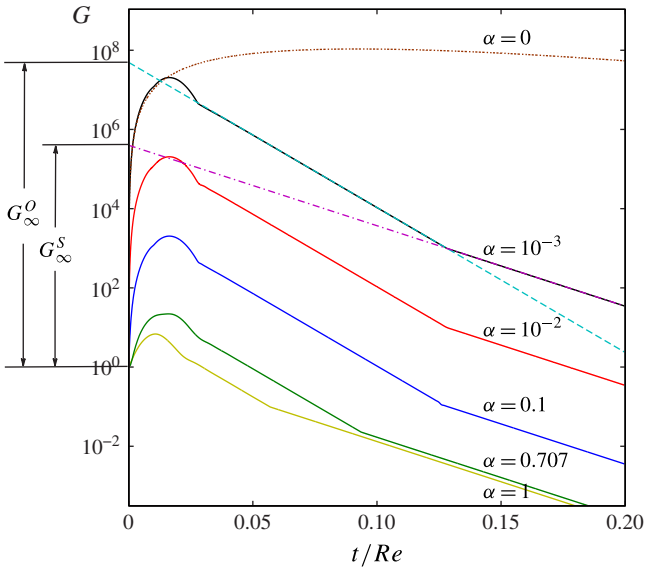


FIGURE 1. (Colour online) Direct computations of optimal gain curves G (solid lines) as a function of t/Re in plane Poiseuille flow at $k = 1$ and $Re_{2D} = 1000$ for $\alpha = 1$, 0.707, 0.1, 10^{-2} and 10^{-3} corresponding respectively, via the Squire transform, to $Re = Re_{2D} = 1000$, 1414.2, 10^4, 10^5 and 10^6. The optimal gain curve for $\alpha = 0$ and $Re = 10^6$ is also presented $(\cdots)$. For $\alpha = 10^{-3}$ (corresponding to $Re = 10^6$), the long-time exponential decay of the leading OS-mode $(- - -)$ and leading SQ-mode $(- \cdot -\cdot)$ are also displayed; they intersect the y-axis at G^O_∞ and G^S_∞, respectively, as given exactly by (7.4) and (7.8).

Figure 2 presents the optimal gain curves of figure 1 but rescaled as $G\left(Re^2_{2D}/\beta^2 Re^2\right)$ in order to verify the predictions of the extended Squire transformation on the large-Re limit for the optimal gain curve at all time derived in § 5. Note that this rescaled gain diverges for the 2D case (when $\beta = 0$) and hence this case is not shown in figure 2. As Re increases, the rescaled optimal gain curves collapse remarkably well onto a single curve. The convergence is so strong that even at $Re/Re_{2D} = 10$ (i.e. $Re = 10^4$, $\alpha = 0.1$), the large-Re asymptote is reached for all t/Re and at $Re/Re_{2D} = \sqrt{2}$ (corresponding to $\alpha = 0.7071$) the asymptotic curve is nearly achieved. Only at very small t/Re, shown in the inset, may a departure of the curve be observed since the new Squire-transformed gain is not valid at the very initial instant where it should converge to unity. This confirms the large-Reynolds-number asymptotics predicted by the Squire transformation on the initial-value problem ((5.15) and (5.19)) for all times larger than unity ($t \gg 1$ but t/Re small, order unity or larger).

The rescaled optimal gain $G\left(Re^2_{2D}/\beta^2 Re^2\right)$ for the case of plane Couette flow at the same $Re_{2D} = 1000$ and $k = 1$ is shown in figure 3. The symbols correspond to the same Reynolds numbers Re and streamwise wavenumber α as in figure 2. The curves are indistinguishable for all Re and α, including $\alpha = 0.707$ corresponding to $Re = 1414.2$. Thus, figures 2 and 3 show that the large-Reynolds-number scaling of optimal growth curves obtained from the extended Squire transformation in § 5 is extremely efficient in predicting the entire optimal gain curve. Also displayed in figure 3 is the long-time exponential decay of the leading OS- and SQ-modes (denoted, respectively, by dashed and dash-dotted lines) for $\alpha = 10^{-3}$ (corresponding to $Re = 10^6$). At $Re_{2D} = 1000$ and $k = 1$, similar to the case of plane Poiseuille flow, the leading eigenmode

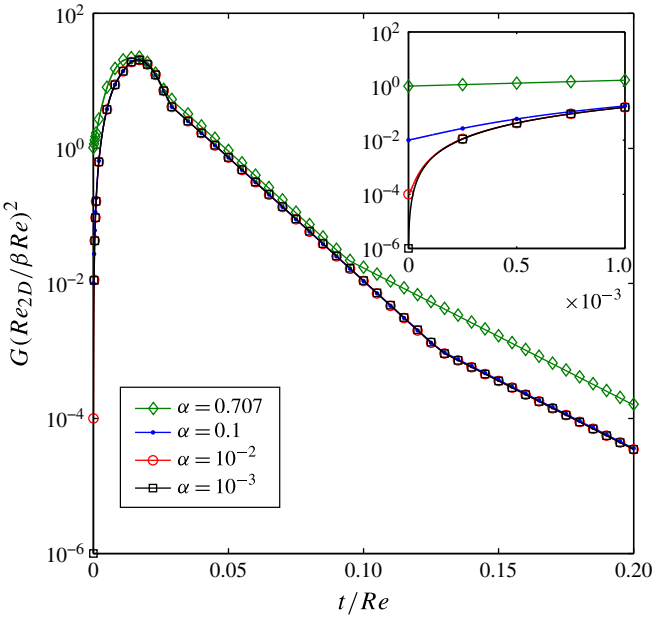


FIGURE 2. (Colour online) Same data as in figure 1 but rescaled according to the large-*Re* prediction via the extended Squire transformation for the optimal gain curve at t/Re finite or large. Note that the curve $\alpha = 1$ (or $\beta = 0$) cannot be plotted in the present scaling. All the cases when $\alpha = 0.1$, $\alpha = 10^{-2}$ and $\alpha = 10^{-3}$ collapse so well for all times that they form a single curve; only in the inset, where the very early instants are shown, is a difference visible since all curves should start at $Re_{2D}^2/\beta^2 Re^2$ for $t = 0$. But even in the close-up plot, the curves for $\alpha = 10^{-2}$ and $\alpha = 10^{-3}$ are indistinguishable except at the very first point at $t = 0$. The curve for $\alpha = 0.707$ is also very close to the large-*Re* asymptotic curve and it only departs at large time.

is an SQ-mode (Schmid & Henningson 2001) and the tail of the optimal gain curve (corresponding to $t \gg 1$) could be expected to show two exponential decay rates. But, in this case, the exponential decay rates of the leading OS- and SQ-modes differ only in the third significant digit. Thus, for the optimization times shown in figure 3, the optimal gain curve displays only one exponential decay corresponding to the leading OS-mode.

Note that, for the optimal growth $G(t)$, the large-*Re* rescaling obtained from the extended Squire transformation is similar to that proposed by Gustavsson (1991) who deduced large-*Re* scaling law for maximum optimal gain in plane Poiseuille flow but, here, wall-normal vorticity rescaling comes out naturally from the extended Squire transformation. Moreover, it is illustrated by comparing the results of large-Reynolds-number asymptotics and direct computations that the extended Squire transformation works for the entire optimal growth curve at all time t/Re, whether small, order unity or large.

The variation of the long-time optimal gains, namely, G_∞^O and G_∞^S, for arbitrary Reynolds numbers *Re* is plotted in figure 4(*a*). The curves are obtained via (7.4) and (7.8) for the various 2D Reynolds numbers $Re_{2D} = 10^2$, $Re_{2D} = 10^3$ and $Re_{2D} = 10^4$ at $k = 1$. The large and small symbols represent G_∞^S and G_∞^O, respectively, directly computed using SVD in plane Poiseuille flow as in figure 1. The long-time gains at

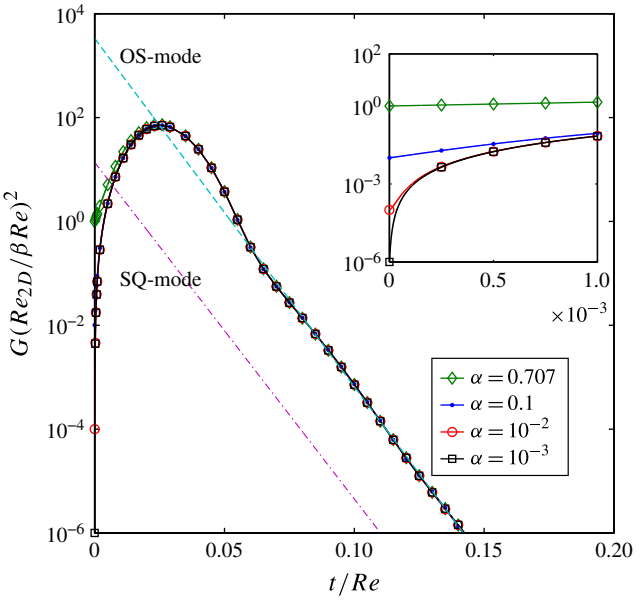


FIGURE 3. (Colour online) Same as figure 2 but for the case of plane Couette flow ($k = 1$ and $Re_{2D} = 1000$). The long-time exponential decay of the leading OS-mode ($- - -$) and leading SQ-mode ($- \cdot -\cdot$) for the case of $\alpha = 10^{-3}$ (corresponding to $Re = 10^6$) is also displayed; they intersect the y-axis at $G^O_\infty \left(Re^2_{2D}/(\beta^2 Re^2)\right)$ and $G^S_\infty \left(Re^2_{2D}/(\beta^2 Re^2)\right)$, respectively.

all Reynolds numbers are precisely predicted by the analytical formulae (7.4) and (7.8). As already observed in figure 1, G^O_∞ is always larger than G^S_∞ in plane Poiseuille flow. Both gains, however, increase with Reynolds number Re and vary as Re^2 at large Reynolds numbers. It is observed that G^S_∞ does not change with respect to the 2D Reynolds number in the range considered: $Re_{2D} = 10^2$, 10^3 and 10^4 (see Appendix for details). Similarly, in the case of plane Couette flow, figure 5(*a*) compares the long-time optimal gains G^O_∞ and G^S_∞ obtained via (7.4) and (7.8) with that directly computed using SVD as in figure 1 over various Re_{2D}. Here, again the analytical formulae (7.4) and (7.8) predict exactly the long-time gains. Also, G^O_∞ is always larger than G^S_∞. However, unlike the case for plane Poiseuille flow, not only G^S_∞ but also G^O_∞ does not vary much for a wide range of 2D Reynolds number (see table 1 for details).

In figures 4(*b*) and 5(*b*), the maximum optimal gain G_{max} (closed symbols) obtained via SVD is compared with the long-time optimal gains G^O_∞ and G^S_∞ (using (7.4) and (7.8)) for various Reynolds numbers Re at fixed 2D Reynolds numbers Re_{2D}. All the data are computed for $k = 1$. When $\beta = 0$, G_{max} is precisely the maximum transient growth corresponding to the 2D Orr mechanism. For a given Re_{2D} and k, both figures 4(*b*) and 5(*b*) show that this value of G_{max} is approximately constant as long as $\beta < 1/\sqrt{2}$ (or $\beta Re/Re_{2D} < 1$). However, when $\beta \to k$ (or $Re/Re_{2D} \gg 1$), G_{max} increases steeply as $(Re/Re_{2D})^2$. Note that at this regime G_{max} corresponds to the 3D lift-up mechanism. When G_{max} is compared with the corresponding long-time extra-gains G_∞, it is seen that they follow the same trend with respect to $\beta Re/Re_{2D}$ in both plane Poiseuille and plane Couette flows. When Re_{2D} is small, G_{max} corresponding to the lift-up mechanism shows large deviations from G^O_∞ at all $\beta Re/Re_{2D}$. However, as $Re_{2D} \gg 1$, G_{max} seems to converge remarkably well toward G^O_∞ at large $\beta Re/Re_{2D}$. This result

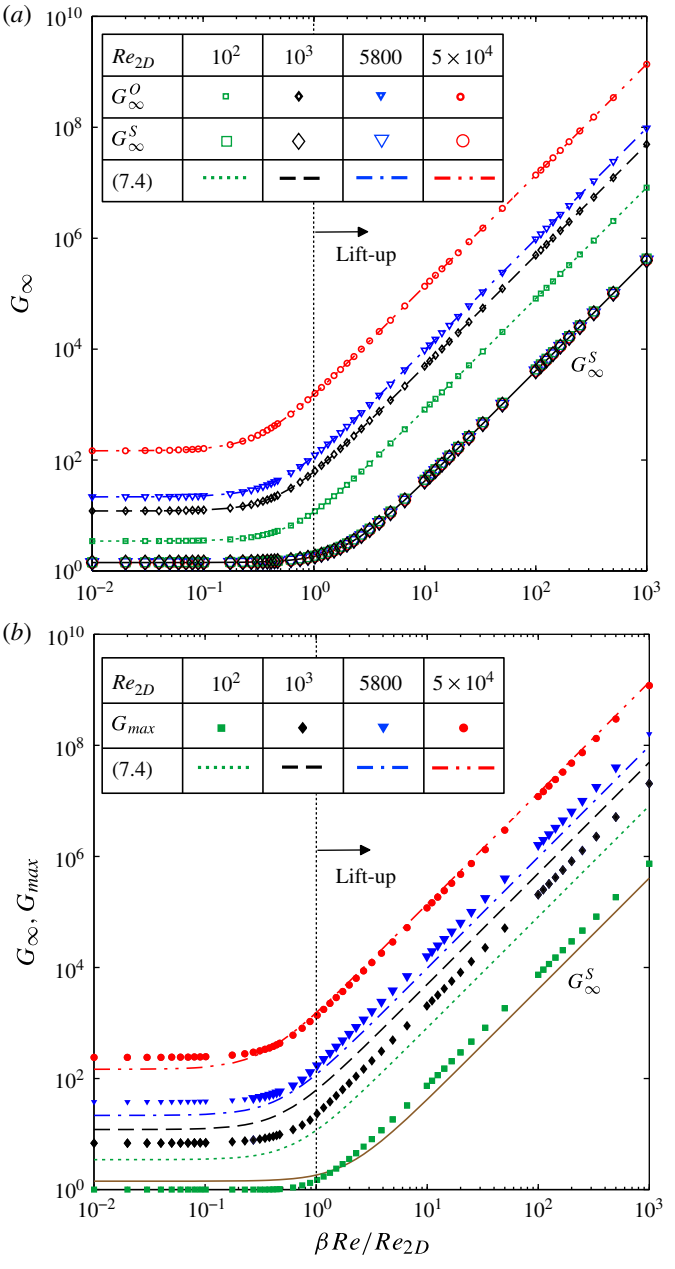


FIGURE 4. (Colour online) (*a*) Long-time asymptotic predictions of the extended Squire transformation for the extra gain for all Reynolds numbers in plane Poiseuille flow is presented here by comparing results obtained via direct computations of the optimal long-time gains G^O_∞ (small symbols) and G^S_∞ (large symbols) as in figure 1 against the analytical formulae (7.4) and (7.8) for G^O_∞ (broken lines) and G^S_∞ (solid line), respectively, when $k = 1$. The prediction of (7.8) is represented by the same solid line since G^{S2D}_∞ and G^{S3D}_∞ are identical at all Re_{2D} considered (see table 1). (*b*) Comparison between the maximum optimal growth G_{max} (closed symbols) and the optimal long-time gains G_∞ over various Re_{2D}. Both G_∞ and G_{max} curves show the same trend but G_{max} is approximately given by G^O_∞ at large Re_{2D}.

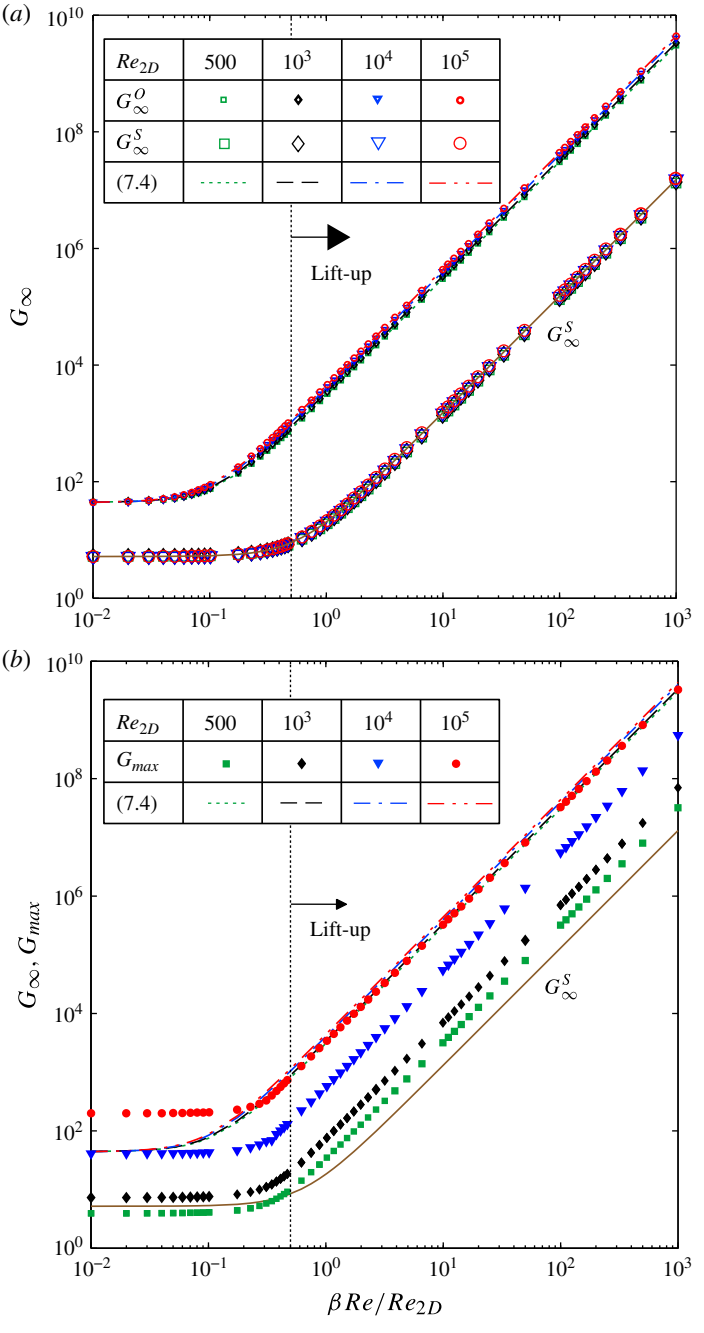


FIGURE 5. (Colour online) Same as figure 4 but for the case of plane Couette flow ($k = 1$).

is important as it shows that, at the large-Reynolds-number limit, the optimal gain is predicted by G^O_∞ and is therefore the product of the 2D Orr mechanism and a lift-up contribution as given by (7.4). This result is in accordance with Farrell & Ioannou (1993) who showed, in viscous constant-shear flows, that arbitrary 3D perturbations

grow with a combination of the lift-up mechanism and the Orr mechanism of the wall-normal velocity. Our results for both plane Poiseuille and plane Couette flow indicate that this amplification process can be universal. And the interaction of the Orr mechanism with the lift-up mechanism determines the optimal growth.

8.2. *Gustavsson's large-Reynolds-number scaling*

Gustavsson (1991) studied the effect of wall-normal velocity forcing on the equation governing the wall-normal vorticity $\tilde{\eta}(y, t)$: the inhomogeneous Squire equation. In particular, Gustavsson (1991) analysed the initial-value problem of $\tilde{\eta}(y, t)$ alone when the initial wall-normal vorticity is zero, i.e. $\tilde{\eta}_0 = 0$, and the initial wall-normal velocity is an eigenfunction of the Orr–Sommerfeld equation (2.3), i.e. $\tilde{v}_0 = \hat{v}_j^O$. While doing so, Gustavsson (1991) and later, Reddy & Henningson (1993) who as opposed to vorticity growth, directly computed the optimal energy growth in plane Poiseuille and plane Couette flows, obtained large-Reynolds-number scaling for G_{max} by rescaling the wall-normal vorticity as

$$\tilde{\eta}(y, t; \alpha, \beta, Re) = \beta Re\, \bar{\eta}(y, t/Re; k, \alpha Re). \tag{8.1}$$

Note that this is equivalent to the extended Squire transformation § 3; however, in the case of Gustavsson (1991) and Reddy & Henningson (1993) this rescaling introduces $(\beta Re)^2$ in the energy norm:

$$\|\tilde{\boldsymbol{q}}\|^2 = \frac{1}{2}\int_{-1}^{1}\left[\left(|\tilde{v}|^2 + \frac{1}{k^2}|\mathrm{D}\tilde{v}|^2\right) + (\beta Re)^2\frac{1}{k^2}|\bar{\eta}|^2\right]\mathrm{d}y, \tag{8.2}$$

which, at $Re \gg 1$, implies that the optimal growth is dominated by the wall-normal vorticity growth

$$G(t; \alpha, \beta, Re) \sim (\beta Re)^2 \sup_{\forall \tilde{v}_0 \neq 0, \tilde{\eta}_0 = 0}\left[\frac{E_{\bar{\eta}}(t/Re; k, \alpha Re)}{E_{\tilde{v}}(0)}\right], \tag{8.3}$$

where

$$E_{\bar{\eta}}(t/Re; k, \alpha Re) = \frac{1}{2}\int_{-1}^{1}\frac{1}{k^2}|\bar{\eta}|^2\,\mathrm{d}y, \tag{8.4}$$

$$E_{\tilde{v}}(0) = \frac{1}{2}\int_{-1}^{1}\left(|\tilde{v}_0|^2 + \frac{1}{k^2}|\mathrm{D}\tilde{v}_0|^2\right)\mathrm{d}y. \tag{8.5}$$

In the present analysis, however, we have applied the Squire transformation on both the Orr–Sommerfeld and Squire eigenfunctions. In addition, the extended Squire transformation is used on the initial-value problem (2.2) for arbitrary initial conditions, in order to derive asymptotic solutions at $Re \gg 1$ and exact optimal gains at large time with the reported effect on the 2D Orr mechanism and the 3D lift-up mechanism. Thus, the extended Squire transformation gives an alternative proof of Gustavsson's scaling for arbitrary αRe as $Re \to \infty$.

8.3. *Extension to confined shear flows with destabilizing temperature gradient*

For the sake of simplicity, let us consider the so-called Rayleigh–Bénard–Poiseuille flow which is simply a channel flow with a constant temperature gradient (see for instance, Nicolas 2002; Jerome *et al.* 2012). Nonetheless, the following analysis is true for arbitrary base-flow temperature distributions. In general, the governing equations of the perturbation field (2.2) can be re-written in terms of the wall-normal velocity $\tilde{v}(y,\, t;\, \alpha,\, \beta,\, Re,\, Ra,\, Pr)$, temperature $\tilde{\theta}(y,\, t;\, \alpha,\, \beta,\, Re,\, Ra,\, Pr)$ and the wall-normal vorticity $\tilde{\eta}(y, t; \alpha, \beta, Re, Ra, Pr)$ at each wave vector $\boldsymbol{k} = (\alpha,\, \beta)^{\mathrm{T}}$ (Chandrasekhar 1961; Joseph 1976; Drazin & Reid 1981; Jerome *et al.* 2012):

$$-\frac{\partial}{\partial t}\begin{bmatrix} k^2 - \mathrm{D}^2 & 0 & 0 \\ 0 & 1 & 0 \\ 0 & 0 & 1 \end{bmatrix}\begin{bmatrix} \tilde{v} \\ \tilde{\theta} \\ \tilde{\eta} \end{bmatrix} = \begin{bmatrix} L_{OS} & -k^2 Ra/\left(Re^2 Pr\right) & 0 \\ \frac{\mathrm{d}\Theta_0}{\mathrm{d}y} & L_{LHE} & 0 \\ \mathrm{i}\beta\frac{\mathrm{d}U_0}{\mathrm{d}y} & 0 & L_{SQ} \end{bmatrix}\begin{bmatrix} \tilde{v} \\ \tilde{\theta} \\ \tilde{\eta} \end{bmatrix}, \tag{8.6}$$

with $\mathrm{D} = \partial/\partial y$ and $k^2 = \alpha^2 + \beta^2$ as in the previous case. Here, $Ra = \alpha^* g l^3 \Delta T/\nu^* \kappa^*$ is the Rayleigh number and $Pr = \nu^*/\kappa^*$ is the Prandtl numbers with g the acceleration due to gravity, ν^* the kinematic viscosity, κ^* the thermal diffusion coefficient and α^* the thermal expansion coefficient. Under the Boussinesq approximation, these parameters are functions of only Θ^*, the average non-dimensional temperature of the channel (and hence, they do not depend on the temperature of the flow field). The space, time, velocity and temperature variables have been non-dimensionalized with respect to the characteristic length scale l, time scale l/U, velocity scale U and temperature scale $\Delta T/2$, respectively. In the case of plane Poiseuille flow with constant cross-stream temperature gradient, l is the half-channel width $h/2$, U is the velocity at the centre of the channel and ΔT is the difference in temperature between the lower and upper wall. Equations (8.6) form the linearized Oberbeck–Boussinesq system of equations (*LOB*) wherein the operators L_{OS} and L_{SQ} are the usual Orr–Sommerfeld and Squire operators, given by (2.3) and (2.4). Whereas, the operator L_{LHE} given by

$$L_{LHE} = \mathrm{i}\alpha U_0 + \frac{1}{RePr}\left(k^2 - \mathrm{D}^2\right) \tag{8.7}$$

comes from the linearized heat equation and it is the advection–diffusion operator governing the evolution of the temperature perturbation. These equations are to be solved for the boundary conditions: $\tilde{v}(\pm 1,\, t) = 0$, $\mathrm{D}\tilde{v}(\pm 1,\, t) = 0$, $\tilde{\eta}(\pm 1,\, t) = 0$ and $\tilde{\theta}(\pm 1, t) = 0$. Here, the wall-normal velocity and temperature perturbations are coupled via the buoyancy terms whereas the wall-normal vorticity equation is decoupled from the temperature perturbations. The Squire equation is, however, forced by the solution of the coupled operator governing the wall-normal velocity and temperature perturbations.

For confined shear flows, the spectrum of (8.6) is discrete and complete (Herron 1980) and it consists of two families of modes, namely, the Orr–Sommerfeld–Oberbeck–Boussinesq (OSOB) eigenfunctions $[\hat{v}_j^O,\, \hat{\theta}_j^O,\, \hat{\eta}_j^O]^{\mathrm{T}}$ and the Squire (SQ) eigenfunctions $[0,\, 0,\, \hat{\eta}_j^S]^{\mathrm{T}}$ with corresponding eigenvalues $\{\lambda_j^O\}$ and $\{\lambda_j^S\}$, respectively. They depend on α, β, Re, Ra and Pr. When $Ra > 1707.78$, the longitudinal OSOB-modes are destabilized as in the classical Rayleigh–Bénard convection.

For every given Ra and Pr, the extended Squire transformation then relates oblique modes with $\alpha \neq 0$, $\beta \neq 0$ at Reynolds number Re to a 2D spanwise-uniform mode

with $\alpha_{2D} = k$, $\beta_{2D} = 0$ at a smaller Reynolds number $Re_{2D} = (\alpha/k)\,Re$:

$$\lambda_j^O(\alpha, \beta, Re, Ra, Pr) = \frac{Re_{2D}}{Re}\lambda_j^{O2D}(k, Re_{2D}, Ra, Pr), \tag{8.8}$$

$$\hat{v}_j^O(y; \alpha, \beta, Re, Ra, Pr) = \hat{v}_j^{O2D}(y; k, Re_{2D}, Ra, Pr), \tag{8.9}$$

$$\hat{\theta}_j^O(y; \alpha, \beta, Re, Ra, Pr) = \frac{Re}{Re_{2D}}\hat{\theta}_j^{O2D}(y; k, Re_{2D}, Ra, Pr), \tag{8.10}$$

$$\hat{\eta}_j^O(y; \alpha, \beta, Re, Ra, Pr) = \frac{\mathrm{i}\beta Re}{Re_{2D}}\hat{\eta}_j^{O2D}(y; k, Re_{2D}, Ra, Pr), \tag{8.11}$$

in the case of the OSOB-modes, and

$$\lambda_j^S(\alpha, \beta, Re, Ra, Pr) = \frac{Re_{2D}}{Re}\lambda_j^{S2D}(k, Re_{2D}, Ra, Pr), \tag{8.12}$$

$$\hat{\eta}_j^S(y; \alpha, \beta, Re, Ra, Pr) = \hat{\eta}_j^{S2D}(y; k, Re_{2D}, Ra, Pr), \tag{8.13}$$

in the case of the SQ-modes. The superscripts 2D refer to variables of the 2D spanwise-uniform modes.

Using this transformation, the evolution of the perturbations in such flows can be written as

$$\begin{aligned}
&\tilde{\boldsymbol{q}}\,(y, t; \alpha, \beta, Re, Ra, Pr) \\
&= \sum_j A_j^O \exp\left(-\mathrm{i}\lambda_j^{O2D} Re_{2D}\frac{t}{Re}\right)\begin{bmatrix} \hat{v}_j^{O2D} \\ (Re/Re_{2D})\,\hat{\theta}_j^{O2D} \\ (\mathrm{i}\beta Re/Re_{2D})\,\hat{\eta}_j^{O2D}\end{bmatrix} \\
&\quad \times \sum_j \left(\frac{\mathrm{i}\beta Re}{Re_{2D}}B_j^O + B_j^S\right)\exp\left(-\mathrm{i}\lambda_j^{S2D} Re_{2D}\frac{t}{Re}\right)\begin{bmatrix} 0 \\ 0 \\ \hat{\eta}_j^{S2D}\end{bmatrix}.
\end{aligned} \tag{8.14}$$

The Fourier amplitudes $\tilde{\boldsymbol{q}}\,(y, t; \alpha, \beta, Re, Ra, Pr) = [\tilde{v}, \tilde{\theta}, \tilde{\eta}]^{\mathrm{T}}$ are functions of y, t and the control parameters, namely, α, β, Re, Ra and Pr. The coefficients $\{A_j^O\}$, $\{B_j^O\}$ and $\{B_j^S\}$ are complex constants that can be determined from the initial conditions on the state variables in the same manner as in the uniform temperature case, treated (5.2), (5.3) and (5.4).

Note that the wall-normal vorticity $\tilde{\eta}$ in the general solution (8.14) is given by exactly the same equation (5.1) and, hence, it should obey the same scaling laws as in the uniform temperature case. Thus, all the results obtained in § 3 apply equally well in such systems.

The rescaled optimal gain $G_{RB}\,(Re_{2D}/\beta Re)^2$ curves at various Reynolds numbers for the case of Rayleigh–Bénard–Poiseuille flow are given in figure 6. The norm used to define the optimal gain G_{RB} is taken as

$$\|\tilde{\boldsymbol{q}}\|^2 = \frac{1}{2}\int_{-1}^{1}\left[|\tilde{v}|^2 + k^{-2}\left(|\mathrm{D}\tilde{v}|^2 + |\tilde{\eta}|^2\right)\right]\mathrm{d}y + \frac{1}{2}Ra\,Pr\int_{-1}^{1}|\hat{\theta}|^2\mathrm{d}y, \tag{8.15}$$

since this choice for the relative weights of the thermal contribution to the energy is both consistent with the classical choice for the Rayleigh–Bénard problem in the absence of through flow and the classical potential energy for stably stratified flows

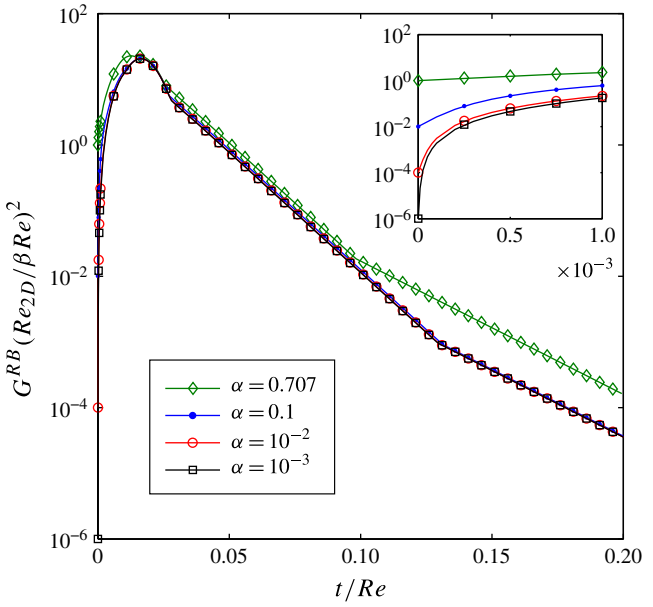


FIGURE 6. (Colour online) Same as figure 2 but for the case of Rayleigh–Bénard–Poiseuille flow at Rayleigh number $Ra = 1000$ and Prandtl number $Pr = 1$. It shows that the large-Reynolds-number asymptotic via the extended Squire transformation is also valid in shear flows with heat addition.

(see Jerome *et al.* 2012 for details). For the results displayed in figure 6, $Ra = 1000$ and $Pr = 1$ are taken along with $Re_{2D} = 1000$ and $k = 1$. The rescaled optimal gain curves are very similar to those in figure 2 corresponding to the uniform termperature case of plane Poiseuille flow. A perfect collapse is observed at all times t/Re, small, order unity or larger, for $\alpha \leqslant 0.1$ or $Re \geqslant 10Re_{2D}$. The mismatch occurs only for times t/Re very small ($<10^{-3}$) as shown in the inset of figure 6. This proves that the large-Re scalings (5.15) and (5.19) derived via the extended Squire transformation are also applicable for confined shear flows with heat addition.

9. Conclusion

The Squire transformation is extended to the wall-normal vorticity component of the Orr–Sommerfeld mode and the Squire mode. By introducing two new fields for the wall-normal vorticity in the 2D case, any 3D eigenmode of the linearized Navier–Stokes equation is thus transformed into a three-component 2D eigenmode with $Re_{2D} = \alpha Re/k$ and $\alpha_{2D} = k$ in wall-bounded parallel flows. Consequently, as a manifestation of the lift-up mechanism, the wall-normal vorticity component in the OS-mode is transformed proportionally to the Reynolds number Re. In wall-bounded parallel flows, this extended Squire transformation allows us to solve the optimal gain at t large but t/Re arbitrary, for any large value of Re with an exact renormalization of the entire gain curve depending only on 2D optimization.

The Squire transformation is extended also to the adjoint eigenmodes. As a consequence, the optimal gain at large time $t \gg (\Delta\omega_{max})^{-1}$, where $\Delta\omega_{max}$ is the difference between the first and second leading eigenmode growth rate, is expressed as an analytical function of $\beta^2 Re^2/Re_{2D}^2$ at a given Re_{2D} and k but arbitrary Re.

	Plane Poiseuille flow				Plane Couette flow			
Re_{2D}	10^2	10^3	5800	5×10^4	500	10^3	10^4	10^5
G_∞^{O2D}	3.4	12	21.6	146.7	44.2	44.2	43.7	43.8
G_∞^{S2D}	1.4	1.4	1.4	1.4	5.2	5.2	5.2	5.2
G_∞^{O3D}	2.4	4.1	4.5	9.4	68.9	75.8	91.6	100
G_∞^{S3D}	0.3	0.28	0.29	0.29	2.5	2.6	2.8	2.9

TABLE 1. Long-time optimal gains for plane Poiseuille and plane Couette flows at various Reynolds numbers Re_{2D}.

If the leading eigenmode is an Orr–Sommerfeld mode, the large-time optimal gain at $t \gg (\Delta\omega_{max})^{-1}$ is shown to be a product of respective gains from the 2D Orr mechanism corresponding to the $\hat{v}$-component of the 2D three-component OS-mode and the contribution of the 3D lift-up mechanism associated with the $\hat{\eta}$-component of the same mode.

The results of these two asymptotic predictions (large Re at arbitrary t/Re and large t but arbitrary Re, respectively) of the extended Squire transformation are verified for the case of plane Poiseuille flow, plane Couette flow and Rayleigh–Bénard–Poiseuille flow by direct numerical computations of optimal gain curves over a wide range of optimization time t. It is observed that, at large Reynolds numbers, the product of the gains from the 2D Orr mechanism and the lift-up mechanism is a good approximation to the maximum optimal transient growth.

Acknowledgements

J.J.S.J. thanks the financial support from the 'Direction des Relations Extérieures' of École Polytechnique. The authors gratefully acknowledge Patrick Huerre, Cristobal Arratia and Yongyun Hwang for many fruitful discussion.

Appendix.

For the case of plane Poiseuille and plane Couette flows, table 1 provides typical values of long-time optimal gains as obtained from (7.4) and (7.8). Here, G_∞^{S2D} and G_∞^{O2D} refer to the long-time optimal gains via 2D mechanisms corresponding to the leading Squire and Orr–Sommerfeld modes, respectively. Similarly, G_∞^{S3D} and G_∞^{O3D} refer to the long-time optimal gains via 3D lift-up mechanisms corresponding respectively to the leading Squire and Orr–Sommerfeld modes. As already seen in figures 4 and 5, the long-time optimal gain G_∞^{S} is always less than G_∞^{O}.

REFERENCES

BAYLY, B. J., ORSZAG, S. A. & HERBERT, T. 1988 Instability mechanisms in shear-flow transition. *Annu. Rev. Fluid Mech.* **20** (1), 359–391.

BOBERG, L. & BROSA, U. 1988 Onset of turbulence in a pipe. *Z. Naturforsch.* **43** (8–9), 697–726.

BUTLER, K. M. & FARRELL, B. F. 1992 Three-dimensional optimal perturbations in viscous shear flow. *Phys. Fluids* A **4** (8), 1637–1650.

CHANDRASEKHAR, S. 1961 *Hydrodynamic and Hydromagnetic Stability*. Dover.

DIPRIMA, R. C. & HABETLER, G. J. 1969 A completeness theorem for non-selfadjoint eigenvalue problem in hydrodynamic stability. *Arch. Rat. Mech. Anal.* **89**, 211–228.

DRAZIN, P. G. & REID, W. H. 1981 *Hydrodynamic Stability*. Cambridge University Press.

ELLINGSEN, T. & PALM, E. 1975 Stability of linear flow. *Phys. Fluids* **18** (4), 487–488.

FARRELL, B. F. 1988 Optimal excitation of perturbations in viscous shear flows. *Phys. Fluids* **31** (8), 2093–2102.

FARRELL, B. F. & IOANNOU, P. J. 1993 Optimal excitation of three-dimensional perturbations in viscous constant shear flow. *Phys. Fluids* A **5**, 1390.

GUSTAVSSON, L. 1991 Energy growth in three-dimensional disturbances in plane Poiseuille flow. *J. Fluid Mech.* **224**, 241–260.

GUSTAVSSON, L. H. & HULTGREN, L. S. 1980 A resonant mechanism in plane Couette flow. *J. Fluid Mech.* **98**, 149–159.

HERBERT, T. 1988 Secondary instability of boundary layers. *Annu. Rev. Fluid Mech.* **20** (1), 487–526.

HERRON, I. H. 1980 A completeness observation on the stability equations for stratified viscous shear flows. *Phys. Fluids* **23**, 836–837.

HULTGREN, L. S. & GUSTAVSSON, L. H. 1981 Algebraic growth of disturbances in a laminar boundary layer. *Phys. Fluids* **24** (6), 1000–1004.

JEROME, J. J. S., CHOMAZ, J.-M. & HUERRE, P. 2012 Transient growth in Rayleigh–Bénard-Poiseuille/Couette convection. *Phys. Fluids* **24** (4), 044103.

JOSEPH, D. D. 1976 *Stability of Fluid Motions I*. Springer.

KACHANOV, Y. S. 1994 Physical mechanisms of laminar-boundary-layer transition. *Annu. Rev. Fluid Mech.* **26** (1), 411–482.

KENDALL, J. M. 1985 Experimental study of disturbances produced in a pre-transitional laminar boundary layer by weak freestream turbulence. *AIAA Paper*.

KLEBANOFF, P. S. 1971 Effects of free-stream turbulence on a laminar boundary layer. *Bull. Am. Phys. Soc.* **16**.

KLEBANOFF, P. S., TIDSTROM, K. D. & SARGENT, L. M. 1962 The three-dimensional nature of boundary-layer instability. *J. Fluid Mech.* **12**, 1–34.

LANDHAL, M. T. 1980 A note on the algebraic instability of inviscid parallel shear flows. *J. Fluid Mech.* **98**, 243–251.

LIN, C. C. 1955 *The Theory of Hydrodynamic Stability*. Cambridge University Press.

MATSUBARA, M. & ALFREDSSON, P. H. 2001 Disturbance growth in boundary layers subjected to free-stream turbulence. *J. Fluid Mech.* **430**, 149–168.

MOFFATT, K. H. 1967 The interaction of turbulence with strong wind shear. In *Proceedings of URSI-IUGG Colloquium on Atmospheric Turbulence and Radio Wave Propagatio* (ed. A. M. Yaglom & Tatarsk), pp. 139–154. Nauka.

MORKOVIN, M. V. 1968 Critical evaluation of transition from laminar to turbulent shear layer with emphasis on hypersonically traveling bodies. *AFFDL Tech. Rep.* pp. 68–149.

MORKOVIN, M. V. 1978 Instability, transition to turbulence and predictability. *AGARDograph No. 236, NATO Document*.

MORKOVIN, M. V. 1984 Bypass transition to turbulence and research desiderata. *Transit. Turbines* 161–204.

NICOLAS, X. 2002 Revue bibliographique sur les écoulements de Poiseuille-Rayleigh–Bénard: écoulements de convection mixte en conduites rectangulaires horizontales chauffées par le bas. *Intl J. Therm. Sci.* **41**, 961–1016.

ORR, W. M. F. 1907 The stability or instability of the steady motions of a perfect liquid and of a viscous liquid. *Proc. R. Irish Acad.* A **27**, 9–138.

REDDY, S. C. & HENNINGSON, D. S. 1993 Energy growth in viscous channel flows. *J. Fluid Mech.* **252**, 209–238.

SARIC, W. S., REED, H. L. & KERSCHEN, E. J. 2002 Boundary layer receptivity to freestream disturbances. *Annu. Rev. Fluid Mech.* **34** (1), 291–319.

SCHENSTED, I. V. 1961 Contributions to the theory of hydrodynamic stability. PhD thesis, University of Michigan, Ann Arbor, MI 48109, USA.

SCHLICHTING, H. 1933 Zur entstehung der turbulenz bei der plattenströmung. *Nachr. Akad. Wiss. Göttingen Math.-Phys. Kl.* 181–208.

SCHLICHTING, H. & GERSTEN, K. 2000 *Boundary-Layer Theory*. MacGraw-Hill.

SCHMID, P. J. 2007 Nonmodal stability theory. *Annu. Rev. Fluid Mech.* **39**, 129–162.

SCHMID, P. J. & HENNINGSON, D. S. 2001 *Stability and Transition in Shear Flows*. Springer.

SCHUBAUER, G. B. & SKRAMSTAD, H. K. 1947 Laminar boundary-layer oscillations and stability of laminar flows. *J. Aero. Sci.* **14**, 69–78.

SHANTHINI, R. 1989 Degeneracies of the temporal Orr–Sommerfeld eigenmodes in plane poiseuille flow. *J. Fluid Mech.* **201**, 13–34.

SQUIRE, H. B. 1933 On the stability of 3D disturbances of viscous flow between parallel walls. *Proc. R. Soc. Lond.* A **142**, 621–628.

TOLLMIEN, W. 1929 Über die entstehung der turbulenz. 1. Mitteilung. *Nachr. Akad. Wiss. Göttingen Math.-Phys. Kl.* 21–44.

VITOSHKIN, H., HEIFETZ, E., GELFGAT, A. Y. & HARNIK, N. 2012 On the role of vortex stretching in energy optimal growth of three-dimensional perturbations on plane parallel shear flows. *J. Fluid Mech.* **707**, 369–380.

WALEFFE, F. 1995 Transition in shear flows. nonlinear normality versus non-normal linearity. *Phys. Fluids* **7**, 3060.